FULL PAPER

Molecular Meccano, Part 61[+]

A Photochemically Driven Molecular-Level Abacus

Peter R. Ashton,[a] Roberto Ballardini,[d] Vincenzo Balzani,*[b] Alberto Credi,[b] Klaus Ruprecht Dress,[a] Eléna Ishow,[b] Cornelis J. Kleverlaan,[c] Oldrich Kocian,[a] Jon A. Preece,[a] Neil Spencer,[a] J. Fraser Stoddart,*[a, e] Margherita Venturi,[b] and Sabine Wenger[a, e]

Abstract: A molecular-level abacus-like system driven by light inputs has been designed in the form of a [2]rotaxane, comprising the π-electron-donating macrocyclic polyether bis-*p*-phenylene-34-crown-10 (BPP34C10) and a dumbbell-shaped component that contains 1) a Ru[II] polypyridine complex as one of its stoppers in the form of a photoactive unit, 2) a *p*-terphenyl-type ring system as a rigid spacer, 3) a 4,4′-bipyridinium unit and a 3,3′-dimethyl-4,4′-bipyridinium unit as π-electron-accepting stations, and 4) a tetraarylmethane group as the second stopper. The synthesis of the [2]rotaxane was accomplished in four successive stages. First of all, the dumbbell-shaped component of the [2]rotaxane was constructed by using conventional synthetic methodology to make 1) the so-called "west-side" comprised of the Ru[II] polypyridine complex linked by a bismethylene spacer to the *p*-terphenyl-type ring system terminated by a benzylic bromomethyl function and 2) the so-called "east-side" comprised of the tetraarylmethane group, attached by a polyether linkage to the bipyridinium unit, itself joined in turn by a trismethylene spacer to an incipient 3,3′-dimeth-

yl-4,4′-bipyridinium unit. Next, 3) the "west-side" and "east-side" were fused together by means of an alkylation to give the dumbbell-shaped compound, which was 4) finally subjected to a thermodynamically driven slippage reaction, with BPP34C10 as the ring, to afford the [2]rotaxane. The structure of this interlocked molecular compound was characterized by mass spectrometry and NMR spectroscopy, which also established, along with cyclic voltammetry, the co-conformational behavior of the molecular shuttle. The stable translational isomer is the one in which the BPP34C10 component encircles the 4,4′-bipyridinium unit, in keeping with the fact that this station is a better π-electron acceptor than the other station. This observation raises the question—can the BPP34C10 macrocycle be made to shuttle between the two stations by a sequence of photoinduced electron transfer processes? In order to find an

answer to this question, the electrochemical, photophysical, and photochemical (under continuous and pulsed excitation) properties of the [2]rotaxane, its dumbbell-shaped component, and some model compounds containing electro- and photoactive units have been investigated. In an attempt to obtain the photoinduced abacus-like movement of the BPP34C10 macrocycle between the two stations, two strategies have been employed—one was based fully on processes that involved only the rotaxane components (intramolecular mechanism), while the other one required the help of external reactants (sacrificial mechanism). Both mechanisms imply a sequence of four steps (destabilization of the stable translational isomer, macrocyclic ring displacement, electronic reset, and nuclear reset) that have to compete with energy-wasteful steps. The results have demonstrated that photochemically driven switching can be performed successfully by the sacrificial mechanism, whereas, in the case of the intramolecular mechanism, it would appear that the electronic reset of the system is faster than the ring displacement.

Keywords: electron transfer · molecular devices · molecular switch · photochemistry · redox chemistry · rotaxanes · self-assembly

[a] Prof. J. F. Stoddart, P. R. Ashton, Dr. K. R. Dress, Dr. O. Kocian,
Dr. J. A. Preece, Dr. N. Spencer, Dr. S. Wenger
School of Chemistry, University of Birmingham
Edgbaston, Birmingham, B15 2TT (UK)

[b] Prof. V. Balzani, Dr. A. Credi, Dr. E. Ishow, Prof. M. Venturi
Dipartimento di Chimica "G. Ciamician", Università di Bologna
Via Selmi 2, 40126 Bologna (Italy)
Fax: (+39) 051-209-9456
E-mail: vbalzani@ciam.unibo.it

[c] Dr. C. J. Kleverlaan
Dipartimento di Chimica, Università di Ferrara
via L. Borsari 46, 44100 Ferrara (Italy)

[d] Dr. R. Ballardini
Istituto FRAE-CNR, via Gobetti 101, 40129 (Italy)

[e] Prof. J. F. Stoddart, Dr. S. Wenger
Current address: Department of Chemistry and Biochemistry
University of California, Los Angeles
405 Hilgard Avenue, Los Angeles, CA 90095-1569 (USA)
Fax: (+1) 310-206-1843
E-mail: stoddart@chem.ucla.edu

[+] For Part 60 see: S. J. Cantrill, D. A. Fulton, A. M. Heiss, A. R. Pease,
J. F. Stoddart, A. J. P. White, D. J. Williams, *Chem. Eur. J.* **2000**, *6*, 2274.

Introduction

The concept of a machine at the molecular level is not a new one. Our body can be looked upon as an extremely complex

Abstract in Italian: *Un [2]rotassano potenzialmente adatto a funzionare come pallottoliere molecolare azionato da stimoli luminosi è stato progettato e sintetizzato. Esso è costituito da un etere corona π elettron donatore (BPP34C10) e da un componente lineare contenente 1) un complesso polipiridinico di Ru^II come unità fotoattiva e "stopper" per il macrociclo, 2) uno spaziatore p-terfenilico rigido, 3) un gruppo 4,4′-dipiridinio ed uno 3,3′-dimetil-4,4′-dipiridinio come "stazioni" π elettron accettrici e 4) un gruppo tetraarilmetano come secondo "stopper". La sintesi del [2]rotassano è stata ottenuta in quattro passaggi successivi. In primo luogo è stato preparato il componente lineare; mediante metodologie sintetiche convenzionali sono state ottenute 1) la cosiddetta "regione occidentale", che comprende il complesso di Ru^II legato allo spaziatore p-terfenilico, funzionalizzato con un gruppo bromobenzilico, e 2) la "regione orientale", costituita dal gruppo tetraarilmetano legato all'unità 4,4′-dipiridinio, a sua volta connessa ad un gruppo precursore dell'unità 3,3′-dimetil-4,4′-dipiridinio. In seguito, 3) la regione occidentale e quella orientale sono state fuse mediante una reazione di alchilazione, ottenendo così il componente lineare desiderato; infine, 4) esso è stato fatto reagire con il macrociclo BPP34C10 sotto controllo termodinamico allo scopo di preparare il [2]rotassano. La struttura del rotassano è stata caratterizzata mediante spettrometria di massa e spettroscopia NMR; tali esperimenti hanno anche messo in evidenza, assieme a misure di voltammetria ciclica, il suo comportamento co-conformazionale. L'isomero traslazionale stabile del rotassano è quello in cui il macrociclo BPP34C10 si trova sull'unità 4,4′-dipiridinio, in accordo con il fatto che questa unità possiede proprietà π elettron accettrici migliori di quella 3,3′-dimetilata. Il quesito cruciale, a questo punto, è: si può spostare il macrociclo BPP34C10 da una stazione all'altra utilizzando una sequenza fotoindotta di processi di trasferimento elettronico? Per rispondere a questa domanda sono state studiate le proprietà elettrochimiche, fotofisiche e fotochimiche (con eccitazione sia continua che pulsata) del [2]rotassano, dei suoi componenti molecolari e di alcuni composti modello per le unità fotoattive ed elettroattive in questione. Sono state esplorate due strategie allo scopo ottenere il movimento fotoindotto del macrociclo da una stazione all'altra del componente lineare: la prima basata su processi coinvolgenti soltanto i componenti del rotassano (meccanismo intramolecolare), la seconda, invece, assistita dall'intervento di reagenti esterni (meccanismo sacrificale). Entrambi i meccanismi implicano una sequenza di quattro eventi (destabilizzazione dell'isomero traslazionale stabile, spostamento del macrociclo, ripristino elettronico e ripristino nucleare), che debbono competere con processi dissipativi. I risultati dimostrano che questo congegno molecolare può essere effettivamente azionato dalla luce utilizzando il meccanismo sacrificale; nel caso del meccanismo intramolecolare, invece, sembra che il ripristino elettronico del sistema sia più rapido dello spostamendo del macrociclo.*

ensemble of molecular-level machines that power our movements, repair damages, and orchestrate our inner worlds of thought, sense, and emotion.[1] The challenge of constructing artificial molecular machines was posed for the first time by Feynman[2] in his famous address entitled "*There is Plenty of Room at the Bottom*" to the American Physical Society in 1959. In his address, he raised a number of interesting issues, such as, "What are the possibilities of small but movable machines?.. An internal combustion engine of molecular size is impossible.. Other chemical reactions, liberating energy when cold, can be used instead.. What would be the utility of such machines?.."

Although some intriguing examples of simple molecule-level machines (e.g., a phototweezer) were reported[3] in the 1980s, it is only in the last few years, thanks to the rapid growth of supramolecular chemistry,[4] that the issues raised by Feynman[2] have become hot topics[5] in contemporary scientific research. Catenanes and rotaxanes[6] are providing cogent answers to the first of Feynman's questions. Their unique molecular architectures lend themselves to the occurrence of large amplitude motions by their component parts—a property reminiscent of the movements displayed by the working parts of machines in the macroscopic world. When the motions of the component parts of interlocked molecules can be induced and controlled by external inputs of energy, such exotic chemical systems can be viewed[5e,f,h] as simple molecular machines. As Feynman predicted,[2] the input of external energy to make such machines work has to be a cold chemical reaction. What apparently he did not predict, somewhat amazingly, is the possibility that the required chemical energy can be provided by light excitation by means of a photochemical reaction.[7–19]

Here, we describe the design, synthesis, and machine-like performance of a [2]rotaxane, in which the ring component can be induced by light excitation to move, that is, switch, between two different recognition sites or "stations" of the dumbbell-shaped component (Figure 1). Such a molecule
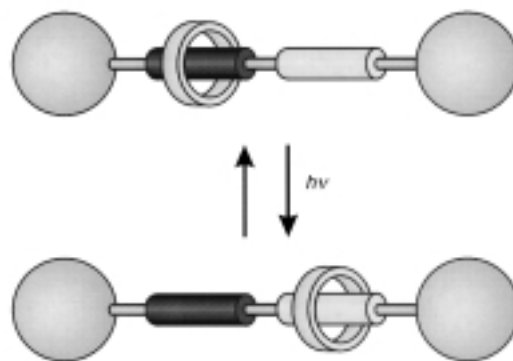

Figure 1. The concept of a photochemically-driven molecular-level abacus.

exhibits an abacus-like geometry and, since it behaves according to binary logic, it could, in principle, be used for information processing[20] at the molecular level. Indeed, molecular-level information processing seems to be a possible answer to Feynman's question about the utility of such "*small but movable machines*".

Design

Just like their macroscopic counterparts, molecular-level machines have to be organized structurally and work as functionally integrated multicomponent systems.[4a, 7, 21, 22] The first step is to produce an accurate design of the working mechanism of the machine, followed by a search for those components that exhibit the required properties, and then finally to find the means to assemble them in the required order. For reasons that will soon become apparent, we have designed a molecular-level machine with the structural features shown in Figure 2a. Since we wanted to use light as
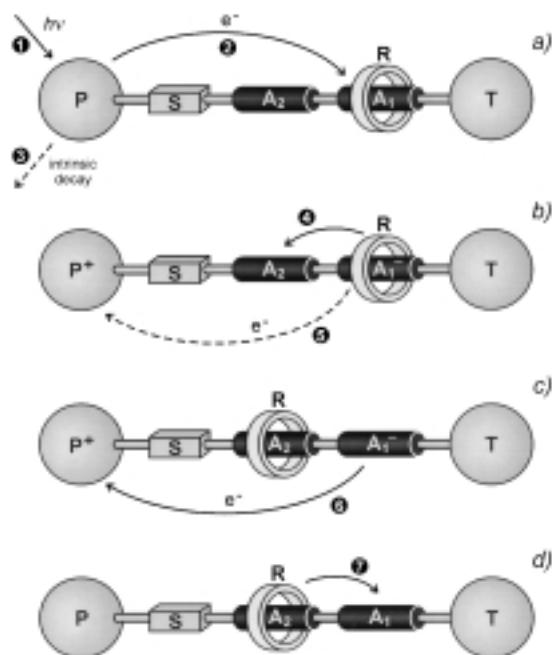
Figure 2. Planned working scheme employing an intramolecular mechanism for the light-driven switching of the ring **R** between the two stations A_1 and A_2. The dashed lines indicate processes that compete with those needed to make the machine work. For more details, refer to the text.

the energy source to make the molecular-level abacus work, we needed to have a photoactive unit **P**. From amongst the various kinds of photoreactions, we chose a photoinduced electron transfer process by which it is possible to affect the strength of donor/acceptor interactions.[7] We then inserted in the dumbbell-shaped component two different π-electron acceptors, A_1 and A_2, which play the role of stations for a π-electron-donor ring **R**. We also decided i) to use **P** as a stopper, ii) to insert a spacer **S** between **P** and the two π-electron acceptors, and iii) to place the better π-electron acceptor A_1 further away from **P** than A_2, that is, place A_1 close to the other stopper **T**. In such a system, the stable translational isomer will be the one in which the π-electron-donating ring **R** encircles the A_1 station. Accordingly, we have devised two working schemes for the photoinduced switching of the ring: one is based entirely on processes that involve only the rotaxane components (intramolecular mechanism) and the other requires the assistance of external reactants (sacrificial mechanism).

Intramolecular mechanism: This mechanism, which is illustrated in Figure 2, is based on the following four operations.

a) *Destabilization of the stable translational isomer*: Light excitation of the photoactive unit **P** (Step 1) should be followed by the transfer of an electron from the excited state to the A_1 station, which is encircled by the ring **R** (Step 2), in order to "deactivate" this station; such a photoinduced electron transfer process has to compete with the intrinsic excited-state decay (Step 3).

b) *Ring displacement*: The ring should move from the reduced station A_1^- to A_2 (Step 4); this step has to compete with the back electron transfer process from A_1^- (still encircled by **R**) to the oxidized photoactive unit P^+ (Step 5).

c) *Electronic reset*: A back electron transfer process from the "free" reduced station A_1^- to P^+ should take place (Step 6) with consequent restoration of the electron-acceptor power to the A_1 station.

d) *Nuclear reset*: As a consequence of the electronic reset, back movement of the ring from A_2 to A_1 should occur (Step 7).

The most important requirement to meet in this intramolecular mechanism is the successful competition of Step 4, which involves complex nuclear movements, with Step 5, which only involves the transfer of an electron. Previous investigations on the shuttling rate of an electron-donating ring between two identical electron-acceptor stations (microsecond timescale)[23] suggests that this requirement is difficult, but not impossible to meet.

Sacrificial mechanism: An alternative, and likely less critical, strategy to obtain the switching process was based on the use of external redox reactants that operate after the photoinduced deactivation of the A_1 station as illustrated in Figure 3. It is based on the following operations.
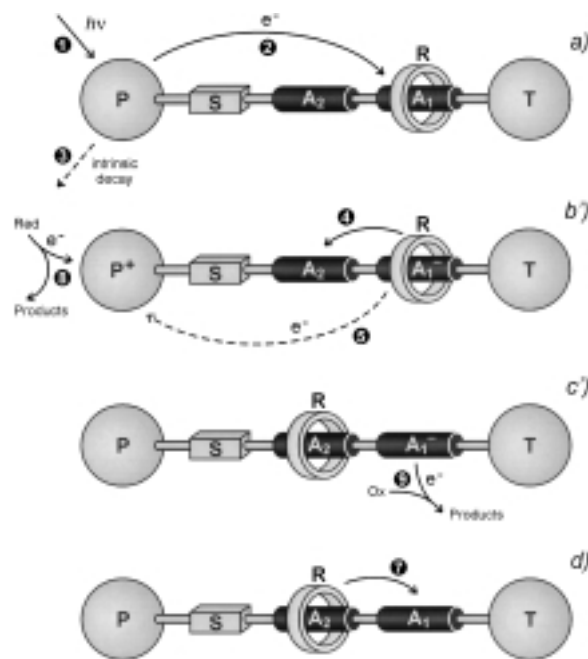

Figure 3. Planned working scheme employing a sacrificial mechanism for the light-driven switching of the ring **R** between the two stations A_1 and A_2. The dashed lines indicate processes that compete with those needed to make the machine work. For more details, refer to the text.

a) *Destabilization of the stable translational isomer*: See the previous mechanism in Figure 2.

b′) *Ring displacement after scavenging of the oxidized photoactive unit*: If the solution contains a suitable reductant **Red**, a fast reaction of **Red** with **P**$^+$ (Step 8) may compete successfully with the back electron transfer reaction (Step 5). In such a case, the displacement of the ring to **A₂** (Step 4), even if it is slow, can take place because the originally occupied station remains in its reduced state **A₁**$^-$.

c′) *Electronic reset*: After an appropriate time, restoration of the electron-acceptor power of the **A₁** station can be obtained by oxidizing **A₁**$^-$ with a suitable oxidant **Ox** (Step 9).

d) *Nuclear reset*: See the previous mechanism in Figure 2.

It is worth noting that the sacrificial strategy has been used extensively to study photoinduced electron transfer processes aimed at solar energy conversion.[24]

Selection of the components and their assembly

On the basis of our experience,[8, 25] we chose (Figure 4) i) a [Ru(bpy)₃]$^{2+}$-type complex as **P**, ii) the π-electron-acceptor 4,4′-bipyridinium unit and its 3,3′-dimethyl analogue as **A₁** and **A₂**, respectively, iii) the π-electron-donating BPP34C10 macrocycle as the ring **R**, iv) a *p*-terphenyl-type ring system as a rigid spacer **S**, and v) a tetraarylmethane group as the
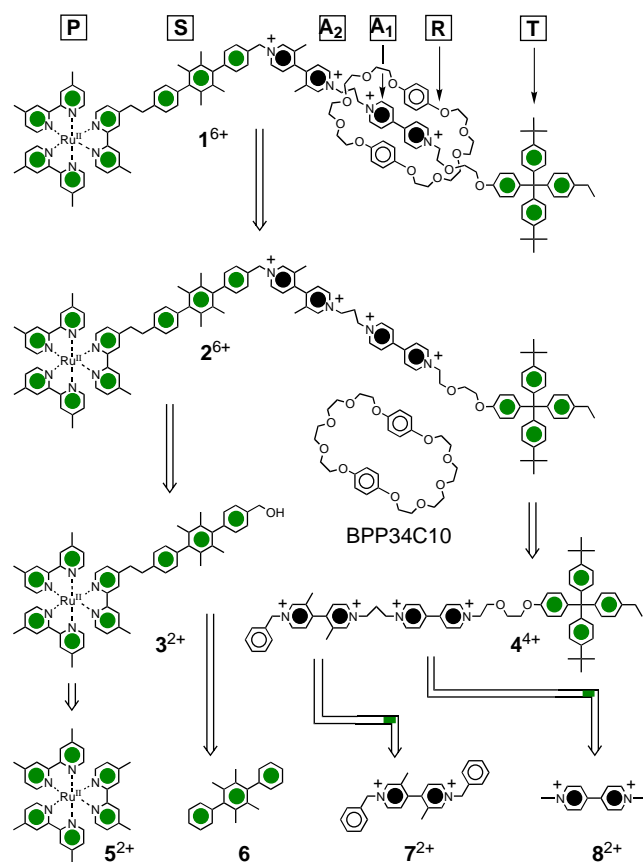

Figure 4. [2]Rotaxane **1**$^{6+}$, its related dumbbell-shaped compound **2**$^{6+}$, the BPP34C10 macrocyclic ring, and some model compounds (**3**$^{2+}$, **4**$^{4+}$, **5**$^{2+}$, **6**, **7**$^{2+}$, and **8**$^{2+}$) of the units present in the dumbbell-shaped component.

second stopper **T**. The reasons why we selected these particular units will become more apparent and easier to appreciate after a discussion of their electrochemical, photophysical, and photochemical properties. Besides the [2]rotaxane **1**$^{6+}$ and its two components, the dumbbell-shaped compound **2**$^{6+}$ and the macrocyclic polyether BPP34C10, Figure 4 also features some model compounds (**3**$^{2+}$ to **8**$^{2+}$) that have been investigated for the sake of comparisons. The "supramolecular" properties of the [2]rotaxane **1**$^{6+}$ depend, of course, not only on the characteristics of the separate components, but also on the co-conformational[26] properties of the multicomponent system. In the case of the intramolecular mechanism (Figure 2), we wanted to decrease as much as possible the rate of the back electron transfer process (Step 5) in order to favor the occurrence of the relatively slow nuclear movements involved in the displacement of the ring from the reduced station to the other one (Step 4). We have attempted to meet this requirement i) by increasing, as much as possible, the exergonicity of the back electron transfer reaction, which is known to be in the Marcus inverted region,[27, 28] and ii) by separating the Ru complex from the π-electron-acceptor stations by a relatively long, rigid, nonplanar spacer. Of course, in doing all this, we had to respond to the requirements of the forward, photoinduced reaction (Step 2), which has to be fast enough to compete with the intrinsic excited-state deactivation (Step 3). In order to reach this goal, the photoinduced reaction should be at least moderately exergonic; also, the distance over which the electron has to be transferred should not be too long. We have attempted to reach a compromise between these contrasting requirements by i) using[29] the [Ru(Me₂bpy)₃]$^{2+}$ complex (**5**$^{2+}$) as the photoactive unit **P**, ii) inserting the nonplanar rod-like component **6** as a rigid spacer **S** between **P** and the bipyridinium **A₁** and **A₂** stations, and iii) positioning the better π-electron accepting unit **A₁** furthest away from **P**. To perform switching by the sacrificial mechanism, we have chosen, as external reactants, triethanolamine (TEOA), which is a very good scavenger of oxidized Ru-polypyridine complexes,[8, 24] and dioxygen, which is commonly used to reoxidize reduced bipyridinium species.[8]

Results and Discussion

Synthesis: The synthesis of the molecular shuttle requires the preparation of two types of components, namely i) a trisbipyridyl complex of ruthenium(II) bearing an almost rigid spacer with, on its terminus, a leaving group that can react efficiently with ii) a trisquaternary salt bearing a bipyridinium unit and a disubstituted pyridylpyridinium moiety. The retrosynthetic analysis of the molecular shuttle is outlined in Scheme 1. This scheme relies on an approach which involves quaternization of a nitrogen by nucleophilic substitution with a ruthenium(II) complex that carries a benzylic bromide function. The synthesis of the [2]rotaxane **1**·6PF₆ is outlined in Schemes 2–4. First of all, the ruthenium(II) complex **9**·2PF₆ (the "west-side") and the tricationic salt **19**·3PF₆ (the "east-side") were synthesized (see Schemes 2 and 3, respectively). Linking the "west-side" with the "east-side" yielded
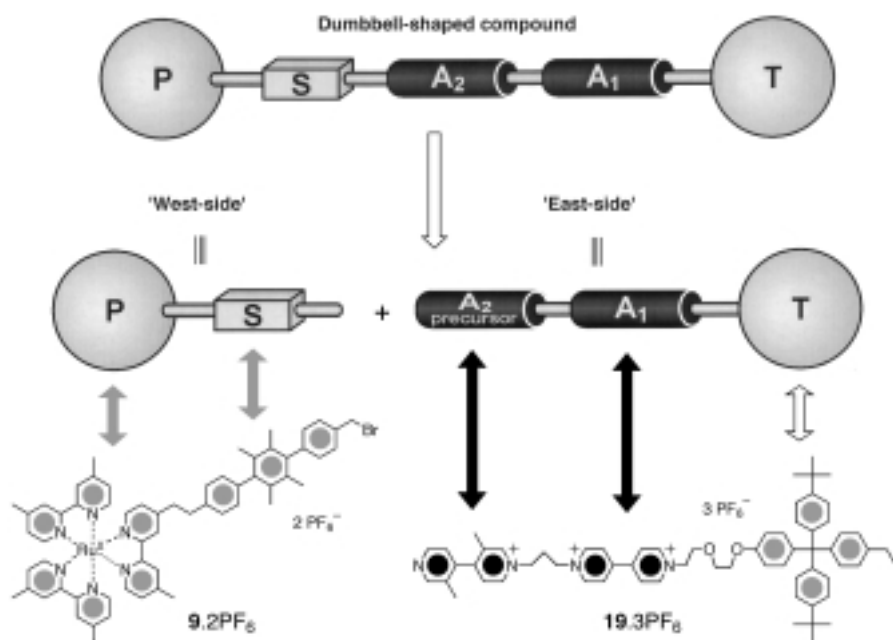
Scheme 1. Retrosynthetic approach for the synthesis of the the dumbbell-shaped compound $2 \cdot 6 PF_6$.

the dumbbell-shaped compound $2 \cdot 6 PF_6$, which incorporates two bipyridinium recognition sites. Finally, the [2]rotaxane $1 \cdot 6 PF_6$ was obtained as a result of a slippage approach[30] to its formation.

Constructing the "west-side": The synthesis of the ruthenium(II) complex $9 \cdot 2 PF_6$ is outlined in Scheme 2. The *tert-*
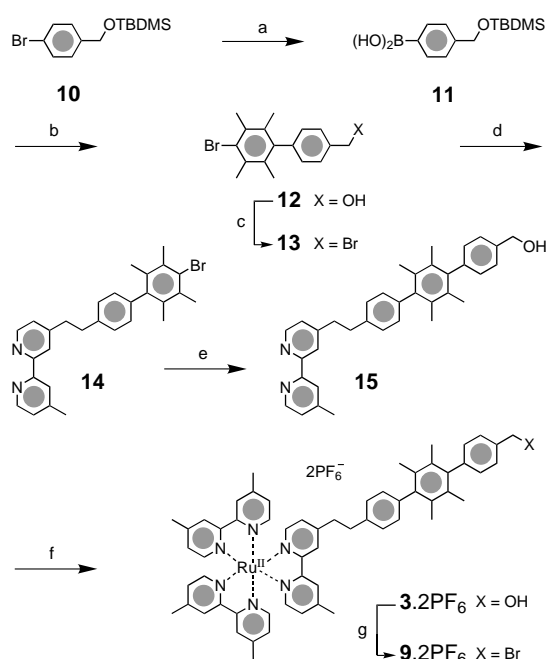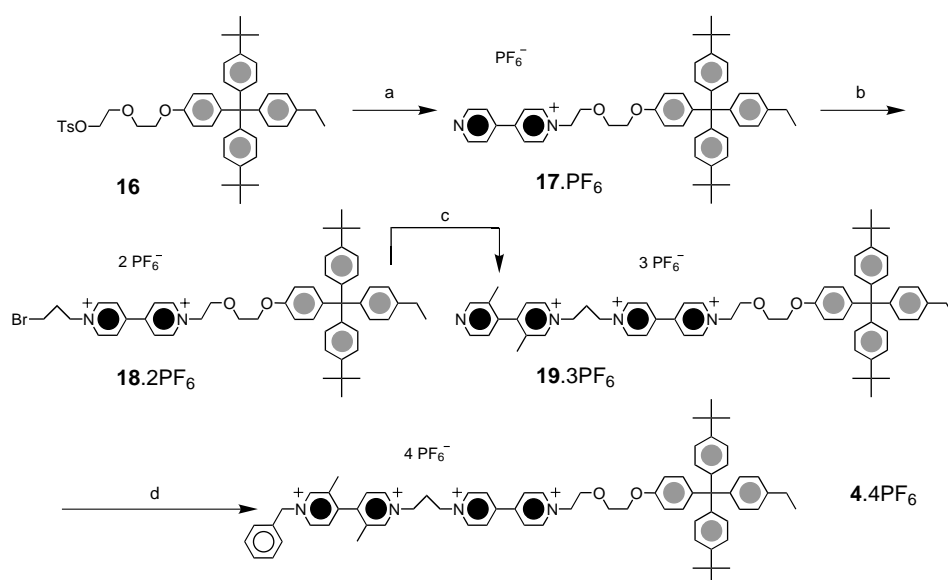

Scheme 2. Synthesis of $9 \cdot 2 PF_6$. Reagents and conditions: a) (1) *n*BuLi/THF, $-78 °C$, 1 h, (2) B(OMe)$_3$, $-78 °C$ to RT, 16 h, (3) 5% HCl, 30 min, 79%; b) (1) 1,4-dibromo-2,3,5,6-tetramethylbenzene/2 M Na$_2$CO$_3$/[Pd-(PPh$_3$)$_4$]/PhCH$_3$/EtOH, reflux, 3 d, (2) TBAF/THF, RT, 12 h, 75%; c) HBr/AcOH (45%w/v), reflux, 12 h, 89%; d) LDA/THF, 78°C to RT, 12 h, 66%; e) (1) 11/2 M Na$_2$CO$_3$/[Pd(PPh$_3$)$_4$]/PhCH$_3$/EtOH, reflux, 3 d, (2) TBAF/THF, RT, 12 h, 62%; f) (1) [Ru(4,4′-dmbpy)$_2$Cl$_2$]/EtOH/H$_2$O, reflux, 24 h, (2) NH$_4$PF$_6$/H$_2$O, RT, 12 h, 66%; g) (1) HBr/AcOH (45%w/v), reflux, 4 h, (2) NH$_4$PF$_6$/H$_2$O, RT, 12 h, 90%.

butyldimethylsilyl *O*-protected 4-bromobenzyl alcohol **10**[31] was transformed in 79% yield into the boronic acid **11** by treatment of the alcohol with *n*BuLi, followed by addition of trimethyl borate in THF at $-78 °C$. The synthesis of the biphenyl derivative **12** was accomplished by Pd^0-catalyzed cross-coupling[32] with an excess of 1,4-dibromo-2,3,5,6-tetramethylbenzene,[33] followed by desilylation with tetrabutylammonium fluoride. The yield for the two steps was 75%. The alcohol **12** then underwent smooth conversion in 89% yield to the corresponding bromide **13** with HBr in acetic acid (45% w/v). Monolithiation of 4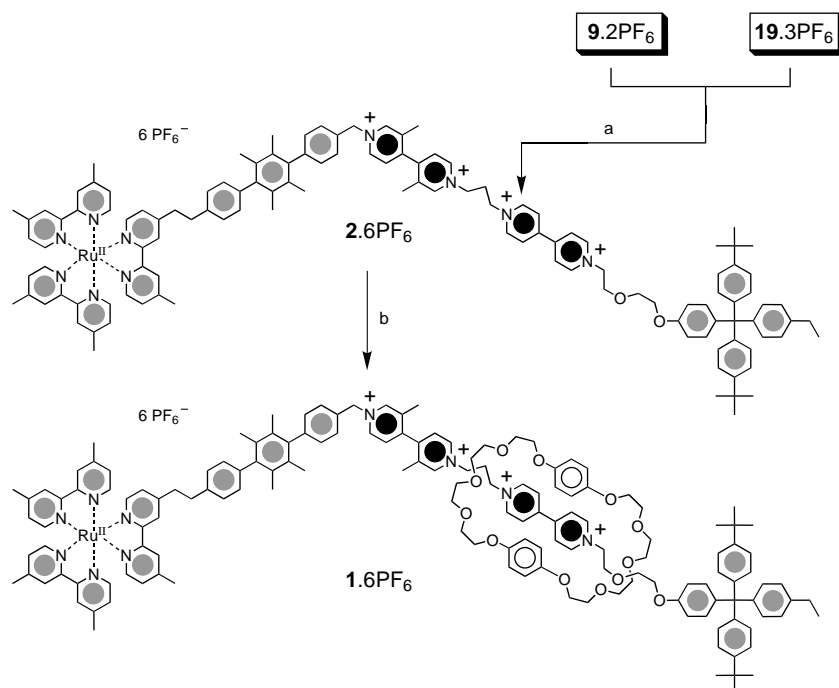,4′-dimethyl-2,2′-bipyridine by using equimolar amounts of LDA[34] in THF, followed by addition of the bromide **13** gave the unsymmetrical substituted bipyridine **14** in 66% yield. A Pd^0-catalyzed cross-coupling reaction between **14** and **11** afforded the bypyridinium-based alcohol **15** in 62% yield. The ruthenium(II) complex $3 \cdot 2 PF_6$ was prepared in 66% yield by treating [Ru(4,4′-dimethyl-2,2′-bipyridine)$_2$]Cl$_2$[35] with the ligand **15** in a mixture of EtOH/H$_2$O, followed by counterion exchange (NH$_4$PF$_6$/H$_2$O/Me$_2$CO). The bromomethyl derivative $9 \cdot 2 PF_6$ was obtained, almost quantitatively, by treatment of the hydroxymethyl derivative $3 \cdot 2 PF_6$ with 45% HBr/AcOH. We found that it is important to prepare the ruthenium(II) complex $3 \cdot 2 PF_6$ prior to the conversion to $9 \cdot 2 PF_6$, as the complexation of ruthenium(II) to the bipyridine ligands protects them from self-alkylation by the reactive benzylic-type bromide function present in compound $9 \cdot 2 PF_6$.

Constructing the "east-side": The synthesis of compound $4 \cdot 4 PF_6$ is outlined in Scheme 3. Compound **16**[36] was treated with an excess of 4,4′-bipyridine in refluxing MeCN in the presence of a catalytic amount of anhydrous LiBr. Following counterion exchange (NH$_4$PF$_6$/H$_2$O/Me$_2$CO), the monoquaternary salt $17 \cdot PF_6$ was isolated in 82% yield. This compound was then alkylated with an excess of 1,3-dibromopropane to afford, after counterion exchange (NH$_4$PF$_6$/H$_2$O), the diquaternary salt $18 \cdot 2 PF_6$ in 69% yield. Following further quaternization of $18 \cdot 2 PF_6$ with an excess of 3,3′-dimethyl-4,4′-bipyridine,[37] the required trisquarternary salt $19 \cdot 3 PF_6$ was isolated in 93% yield after counterion exchange (NH$_4$PF$_6$/H$_2$O). The tetrakisquaternary salt $4 \cdot 4 PF_6$, needed as a model compound in electrochemical studies, was obtained by quaternization of $19 \cdot 3 PF_6$ with benzyl bromide and subsequent counterion exchange (NH$_4$PF$_6$/H$_2$O).

Linking the "west-side" to the "east-side": The ruthenium(II) complex $9 \cdot 2 PF_6$ and the tricationic bipyridinium salt $19 \cdot 3 PF_6$ were reacted together (Scheme 4) in refluxing MeCN to give,

Scheme 3. Synthesis of $\mathbf{4} \cdot 4\,\mathrm{PF}_6$. Reagents and conditions: a) (1) 4,4′-bipyridine/LiBr/MeCN, reflux, 3 d, (2) $\mathrm{NH}_4\mathrm{PF}_6/\mathrm{H}_2\mathrm{O}/\mathrm{Me}_2\mathrm{CO}$, RT, 12 h, 82 %; b) (1) 1,3-dibromopropane/MeCN, reflux, 4 d, (2) $\mathrm{NH}_4\mathrm{PF}_6/\mathrm{H}_2\mathrm{O}/\mathrm{Me}_2\mathrm{CO}$, RT, 12 h, 69 %; c) (1) 3,3′-dimethyl-4,4′-bipyridine/MeCN, reflux, 7 d, (2) $\mathrm{NH}_4\mathrm{PF}_6/\mathrm{H}_2\mathrm{O}$, RT, 12 h, 93 %; d) (1) $\mathrm{PhCH}_2\mathrm{Br}/\mathrm{MeCN}$, reflux, 4 d, (2) $\mathrm{NH}_4\mathrm{PF}_6/\mathrm{H}_2\mathrm{O}$, RT, 12 h, 75 %.

rocyclic polyether instead of BPP34C10, slipping of the crown ether component off the dumbbell component of the corresponding [2]rotaxane[38] was observed.

Mass spectrometry: Liquid secondary ion mass spectrometry (LSIMS) was employed successfully in the characterization of the key compounds $\mathbf{19} \cdot 3\,\mathrm{PF}_6$, $\mathbf{4} \cdot 4\,\mathrm{PF}_6$, $\mathbf{3} \cdot 2\,\mathrm{PF}_6$, $\mathbf{9} \cdot 2\,\mathrm{PF}_6$, the dumbbell-shaped molecule $\mathbf{2} \cdot 6\,\mathrm{PF}_6$, and the [2]rotaxane $\mathbf{1} \cdot 6\,\mathrm{PF}_6$. In all cases, peaks for the successive losses of one, two, or three PF_6^- counterions were observed (Table 1). Additionally, the [2]rotaxane $\mathbf{1} \cdot 6\,\mathrm{PF}_6$ was characterized by electrospray mass spectrometry.

NMR spectroscopy: Compounds $\mathbf{1} \cdot 6\,\mathrm{PF}_6$, $\mathbf{2} \cdot 6\,\mathrm{PF}_6$, $\mathbf{3} \cdot 2\,\mathrm{PF}_6$, $\mathbf{4} \cdot 4\,\mathrm{PF}_6$, $\mathbf{9} \cdot 2\,\mathrm{PF}_6$, $\mathbf{10}-\mathbf{16}$, $\mathbf{17} \cdot \mathrm{PF}_6$, $\mathbf{18} \cdot 2\,\mathrm{PF}_6$, and $\mathbf{19} \cdot 3\,\mathrm{PF}_6$ were characterized by $^1\mathrm{H}$ NMR spectroscopy, which included $^1\mathrm{H}-^1\mathrm{H}$ COSY experiments for full assignments in cases of $\mathbf{1} \cdot 6\,\mathrm{PF}_6$, $\mathbf{2} \cdot 6\,\mathrm{PF}_6$, $\mathbf{4} \cdot 4\,\mathrm{PF}_6$, and $\mathbf{9} \cdot 2\,\mathrm{PF}_6$, and by noise-decoupled $^{13}\mathrm{C}$ NMR spectroscopy. The [2]rotaxane $\mathbf{1} \cdot 6\,\mathrm{PF}_6$ incorporates two different bipyridinium recognition sites, a 4,4′-bipyridinium unit ($\mathbf{A_1}$) and a 3,3′-dimethyl-4,4′-bipyridinium unit ($\mathbf{A_2}$), within the dumbbell-shaped component, but only one BPP34C10 macrocycle. Thus, the macrocyclic component is free to move back and forth from one recognition site to the other depending upon their binding affinities, which can be modified photochemically. The preferential oc-

Scheme 4. Synthesis of the [2]rotaxane $\mathbf{1} \cdot 6\,\mathrm{PF}_6$. Reagents and conditions: a) (1) MeCN, reflux, 6 d, (2) $\mathrm{NH}_4\mathrm{PF}_6/\mathrm{H}_2\mathrm{O}$, RT, 12 h, 63 %; b) (1) BPP34C10/MeCN, 50 °C, 4 d, (2) $\mathrm{NH}_4\mathrm{PF}_6/\mathrm{H}_2\mathrm{O}$, RT, 12 h, 59 %.

after counterion exchange ($\mathrm{NH}_4\mathrm{PF}_6/\mathrm{H}_2\mathrm{O}$), the dumbbell-shaped compound $\mathbf{2} \cdot 6\,\mathrm{PF}_6$ in 63 % yield.

Obtaining the molecular shuttle by slippage: Heating $\mathbf{2} \cdot 6\,\mathrm{PF}_6$ with five equivalents of BPP34C10 in MeCN at 50 °C for four days led (Scheme 4) to the isolation of the [2]rotaxane $\mathbf{1} \cdot 6\,\mathrm{PF}_6$ in 59 % yield as a stable compound, which, upon silica gel column chromatography in $\mathrm{MeOH}/2\;\mathrm{mol\,L}^{-1}\;\mathrm{NH}_4\mathrm{Cl/MeNO}_2$ (7:2:1 v/v/v) as eluent, remained unchanged. However, when 1,5-naphtho-1,4-phenylene-36-crown-10 was used as the mac-

cupation of site $\mathbf{A_1}$ in the ground state was anticipated from previous complexation studies,[39] which demonstrated that the binding affinity of BPP34C10 for a model 4,4′-bipyridinium derivative is about ten times greater than for corresponding 3,3′-dimethyl-4,4′-bipyridinium derivative. The partial $^1\mathrm{H}$ NMR spectroscopic data for the [2]rotaxane $\mathbf{1} \cdot 6\,\mathrm{PF}_6$ and the reference compound—the dumbbell-shaped molecule $\mathbf{2} \cdot 6\,\mathrm{PF}_6$—are listed in Table 2. Significant upfield shifts are observed (Figures 5 and 6) only for the signals arising from the α- and β-protons with respect to the nitrogen atom in the

Table 1. LSIMS data[a] for the bpy-based quaternary salts $19 \cdot 3\,PF_6$ and $4 \cdot 4\,PF_6$, the Ru complexes $3 \cdot 2\,PF_6$ and $9 \cdot 2\,PF_6$, the dumbbell-shaped compound $2 \cdot 6\,PF_6$, and the [2]rotaxane $1 \cdot 6\,PF_6$.

	$[M]^{+[b]}$	$[M-PF_6]^+$	$[M-2PF_6]^+$	$[M-3PF_6]^+$
$19 \cdot 3\,PF_6$	(1365)[c]	1220	1075	929
$4 \cdot 4\,PF_6$	(1600)	1456	1311	1165
$3 \cdot 2\,PF_6$	1294[d]	1127	981	–
$9 \cdot 2\,PF_6$	(1335)	1189	1045	–
$2 \cdot 6\,PF_6$	(2765)	2620	2475	2330
$1 \cdot 6\,PF_6$	3303[e]	3157	3012	2867

[a] LSIMS mass spectra were obtained using a ZabSpec mass spectrometer equipped with a cesium ion source operating at ≈ 30 keV. [b] $M =$ molecular weight. [c] The numbers in parentheses refer to peaks that were not observed. [d] $[M+Na]^+$. [e] $[M+H]^+$.

bipyridinium unit A_I. The resonances for the α- and β-protons are shifted to higher frequencies by approximately 0.24 ppm and 0.50 ppm, respectively, while the signal for the hydroquinone ring protons of BPP34C10 is shifted upfield by 0.52 ppm (Figure 6). These changes in chemical shifts are
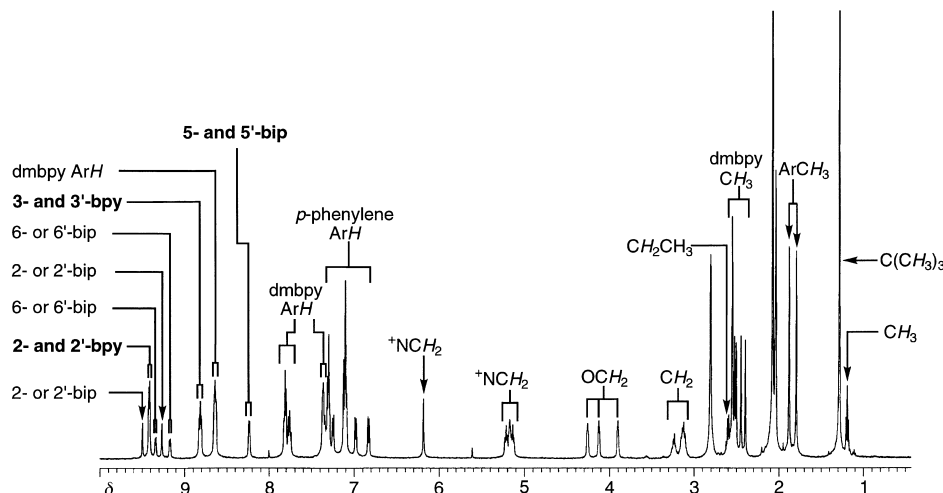
Figure 5. ^{1}H NMR Spectra (500 MHz, CD$_3$COCD$_3$) of the dumbbell-shaped compound $2 \cdot 6\,PF_6$. Note that bip refers to 3,3′-bipicoline and bpy refers to 4,4′-bipyridine. The assignments in bold represent the signals that change their chemical shifts on formation of the [2]rotaxane, $1 \cdot 6\,PF_6$.
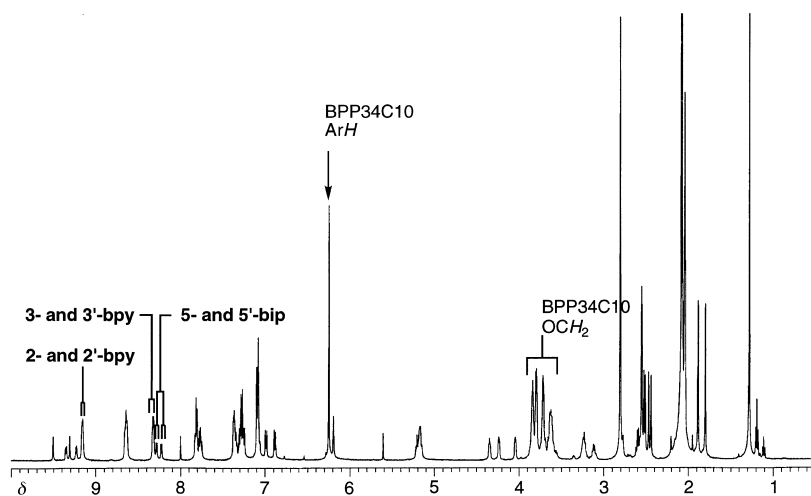
Figure 6. ^{1}H NMR Spectra (500 MHz, CD$_3$COCD$_3$) of the [2]rotaxane $1 \cdot 6\,PF_6$. Note that bip refers to 3,3′-bipicoline and bpy refers to 4,4′-bipyridine. The partial assignments for the signals indicate the formation of the [2]rotaxane.

characteristic of the inclusion of a bipyridinium unit inside a BPP34C10 macrocycle.

Electrochemical behavior: The machine-like behavior of the [2]rotaxane 1^{6+} is based on electron transfer processes that have to bring about the switching of the ring between the two stations of the dumbbell-shaped component. Since i) the occurrence of such processes is related to the electrochemical potentials of the stations and ii) the potential shifts, resulting from donor/acceptor interactions, can yield useful information about the station occupied by the ring along the dumbbell-shaped component, electrochemical features were an integral part of the design of the [2]rotaxane 1^{6+}. Hence, we have investigated the electrochemical behavior of the [2]rotaxane 1^{6+}, the dumbbell-shaped compound 2^{6+}, the BPP34C10 ring, and some of the model compounds shown in Figure 4. The results obtained are summarized in Table 3 and Figure 7.
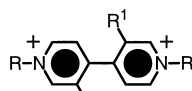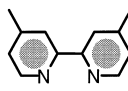
Components: It is well known[36, 38] that the bipyridinium dication 8^{2+} undergoes two reversible one-electron reduction processes. The 3,3′-dimethyl analogue 7^{2+} also undergoes two reversible one-electron reduction processes, but at considerably more negative potential values than 8^{2+} because of the steric hindrance caused by the methyl substituents to the coplanarity of the two pyridinium subunits; this affords a conformation which would favor delocalization of the added electrons.[40] In the wire-type compound 4^{4+}, the reduction processes associated with the two bipyridinium units 7^{2+} and 8^{2+} are clearly distinguishable, even if some shift is observed in the potential values, presumably as a result of the closeness of the positive charges. It should also be noted that 4^{4+} shows a nonreversible oxidation process that can be assigned[36, 38] to the tetraarylmethane stopper. The $[Ru(Me_2bpy)_3]^{2+}$ complex (5^{2+}) displays a metal-localized reversible monoelectronic oxidation process and three ligand-localized reversible monoelectronic reduction processes.[41] The Ru complex 3^{2+}, which is obtained by joining up 5^{2+} with 6, practically behaves just like 5^{2+}. It does not reveal any new process attributable to 6, indicating that this spacer, as expected,[42] does not exhibit any redox activity in the potential window examined.

Table 2. Selected ^{1}H NMR chemical shifts (δ values) in CD$_3$COCD$_3$ at 31 °C for the dumbbell-shaped compound $2\cdot6\,PF_6$ and the [2]rotaxane $1\cdot6\,PF_6$.

Protons	$2\cdot6\,PF_6$	$1\cdot6\,PF_6$	$\Delta\delta$
A_1–α_1/α_2[a]	9.40(d, 2H)/9.37 (d, 2H)	9.16 (d, 2H)/9.14 (d, 2H)	−0.24/−0.23
A_1–β_1/β_2[b]	8.82 (d, 2H)/8.79 (d, 2H)	8.31 (d, 4H)	−0.51/−0.48
A_2–α_1/α_4[c]	9.47 (s, 1H)/9.23 (s, 1H)	9.48 (s, 1H)/9.29 (s, 1H)	+0.01/+0.06
A_2–α_2/α_3[d]	9.31 (d, 1H)/9.14 (d, 1H)	9.32 (d, 1H)/9.21 (d, 1H)	+0.01/+0.07
A_2–β_1/β_2[e]	8.23 (d, 1H)/8.21 (d, 1H)	8.27 (d, 1H)/8.21 (d, 1H)	+0.04/0.00
ArH[f,g]	–	6.25 (s, 8H)	−0.52

[a] Refers to H (2,6/2′,6′). [b] Refers to H (3,5/3′,5′). [c] Refers to H (2/2′). [d] Refers to H (6/6′). [e] Refers to H (5/5′). [f] Refers to protons of the hydroquinone rings incorporated within BPP34C10. [g] The δ value for hydroquinone ring protons of BPP34C10 in CD$_3$COCD$_3$ at ambient temperature is 6.77.

Table 3. Electrochemical data.[a]

	E_{ox} [V][b]			E_{red} [V][b]						
	stopper	crown ether	Ru	R^1=H	Me	H	Me			
8^{2+} (R = Me)					−0.43	−0.84				
7^{2+} (R = Bn)					−0.74		−0.94			
4^{4+}	1.60[c]			−0.36	−0.69	−0.84	−0.97			
BPP34C10		1.23[c] 1.36[c]								
3^{2+}			1.15					−1.43	−1.63	−1.87
2^{6+}	1.60[c]		1.15	−0.36	−0.68	−0.83	−0.96	−1.43	ads.	ads.
1^{6+}	1.70[c]	1.40[c,d]	1.15	−0.44	−0.73	−0.83	−0.99	−1.43	ads.	ads.

[a] Argon purged MeCN, room temperature. [b] Halfwave potential values in V vs. SCE; reversible and monoelectronic processes, unless otherwise indicated. [c] Not fully reversible process; potential value estimated from DPV peaks. [d] Two-electron process.

The BPP34C10 macrocycle is well known to undergo two not fully reversible monoelectronic oxidation processes.[43]

[2]Rotaxane and the dumbbell-shaped compound: In the dumbbell-shaped compound 2^{6+}, all the redox processes of the component units are present at almost the same potentials as in the separated units (Table 3 and Figure 7); this shows that there is no substantial intercomponent electronic interaction. In going from the dumbbell-shaped compound 2^{6+} to the [2]rotaxane 1^{6+}, some processes are affected and others are not. All the processes related to the Ru-based unit, that is, the metal-localized oxidation and the ligand-localized reduction, do not show any appreciable changes. The first reduction of the A_1 unit is displaced noticeably toward more negative potential values, indicating that it is surrounded by the π-electron donating BPP34C10 ring (Figure 8), whose oxidation[44] is displaced accordingly toward more positive potential values. These observations are confirmed by the values of the potential shifts, which are close to those observed for a previously investigated[36] [2]rotaxane that incorporates the BPP34C10 ring and a station similar to A_1. The fact that the ring encircles the A_1 station in the more stable isomer was exactly what we expected, since the A_1 station is a better π-electron acceptor than the A_2 one. The reduction potentials (Table 3) of A_1 and A_2 in the dumbbell-shaped compound 2^{6+} (or of the separated 7^{2+} and 8^{2+} compounds) suggest that the translational isomer of 1^{6+}, shown in Figure 4, is by far more highly populated than the other one, as confirmed by the NMR results. The second reduction wave of 1^{6+}, which corresponds to the first reduction of the A_2 station, is also displaced toward more negative potentials, demonstrating that, at this stage, the A_2 unit is encircled by the BPP34C10 ring. It has to be stressed, however, that this reduction happens after the first reduction of the A_1 station. This behavior confirms that, as we planned to achieve, when the better station (A_1) of the two has been "deactivated", the BPP34C10 ring moves to the alternative A_2 station. Under these conditions, from the values of the first reduction potential of A_2 and the second reduction potential of A_1 in the dumbbell-shaped component (Table 3), it can be estimated that the translational isomer with the BPP34C10 ring encircling A_2 is much more populated than that in which the BPP34C10 ring encircles A_1^-. Also, when the A_2 station has been reduced, the position of the BPP34C10 ring is no longer controlled by strong donor/acceptor interactions; from the electrochemical results, it seems that it resides close to A_2^-. The reversibility of the electrochemical processes involving the two stations shows that, after a two-electron reduction of the [2]rotaxane 1^{6+}, one-electron oxidation relocates the BPP34C10 ring on the A_2 station and a successive one-electron oxidation entices it back again onto the A_1 station. The electrochemical reversibility of these processes indicates that the rates of the electrochemically induced ring movements are faster than the highest scan rate (1 Vs^{-1}) used in the conventional electrochemical experiments. This observation is not surprising since, in a previously studied[23] [2]rotaxane, the shuttling of BPP34C10 between two identical 4,4′-bipyridinium stations was found to occur with a rate constant of 300000 s^{-1} at 298 K, even in the presence of donor/acceptor interactions. In an attempt to obtain the value of the rate constant for ring displacement after the reduction of A_1 (Step 4 in Figures 2 and 3), we have tried to perform experiments at much faster scan rates by using a piece of electrochemical equipment described in the Experimental Section.[45] Unfortunately, these experiments were unsuccessful because of severe adsorption phenomena.

Photochemical and photophysical behavior: In order to effect the photoinduced switching process (Figures 2 and 3) upon rotaxane 1^{6+}, we needed a component **P** that exhibited well-defined spectroscopic and redox properties, namely: i) light absorption in a region of the spectrum at which the other components of the system do not show strong bands, ii)
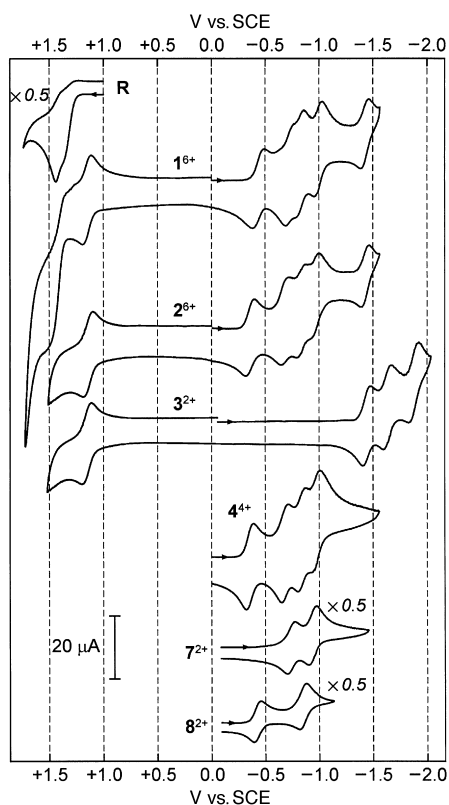
Figure 7. Cyclic voltammetric patterns (MeCN, 298 K, scan rate 200 mV s^{-1}) for the model compounds (3^{2+}, 4^{4+}, 7^{2+}, and 8^{2+}), dumbbell-shaped compound 2^{6+}, the BPP34C10 macrocycle (**R**), and the [2]rotaxane 1^{6+}.

suitable excited-state energy, lifetime, and reducing power, and iii) reversible redox behavior. It is well known that Ru^{II} complexes of polypyridine ligands exhibit[25] outstanding excited state and redox properties and that their photo-induced electron transfer processes with bipyridinium-type compounds are fully reversible.[46] Most relevant to our present objectives are the studies performed[8d, 27, 28] on systems in which [Ru(bpy)$_3$]$^{2+}$ derivatives are covalently linked to bipyridinium units. It has been shown that it is indeed possible to obtain a photoinduced electron transfer from the Ru complex to the bipyridinium unit, and that the rate constants of the forward (photoinduced) and back processes depend upon thermodynamic and kinetic factors, as expected on the basis of Marcus theory.[7, 47]

We have recorded the absorption spectra of all the compounds shown in Figure 4 and we have found that the spectrum of [2]rotaxane 1^{6+} (Figure 9) is substantially that which would be predicted on the basis of contributions from its different chromophoric units. It should be noted that the weak charge transfer band (λ_{max} ca. 450 nm with ε_{max} ca. 500 M^{-1} cm^{-1})[36, 38] arising from the interaction between **A$_1$** and BPP34C10 cannot be observed because it is hidden by the much more intense metal-to-ligand charge transfer (MLCT) band of the Ru-based component 3^{2+} ($\lambda_{max} = 450$ nm with ε_{max} ca. 15 000 M^{-1} cm^{-1})[41] or compound 5^{2+}. Upon excitation of **P** at 450 nm, both the [2]rotaxane 1^{6+} (Figure 9) and the dumbbell-shaped compound 2^{6+} exhibit an emission band at $\lambda_{max} = 618$ nm, which corresponds to that exhibited by the Ru-based compound 3^{2+}.[48] Both the lifetime and emission
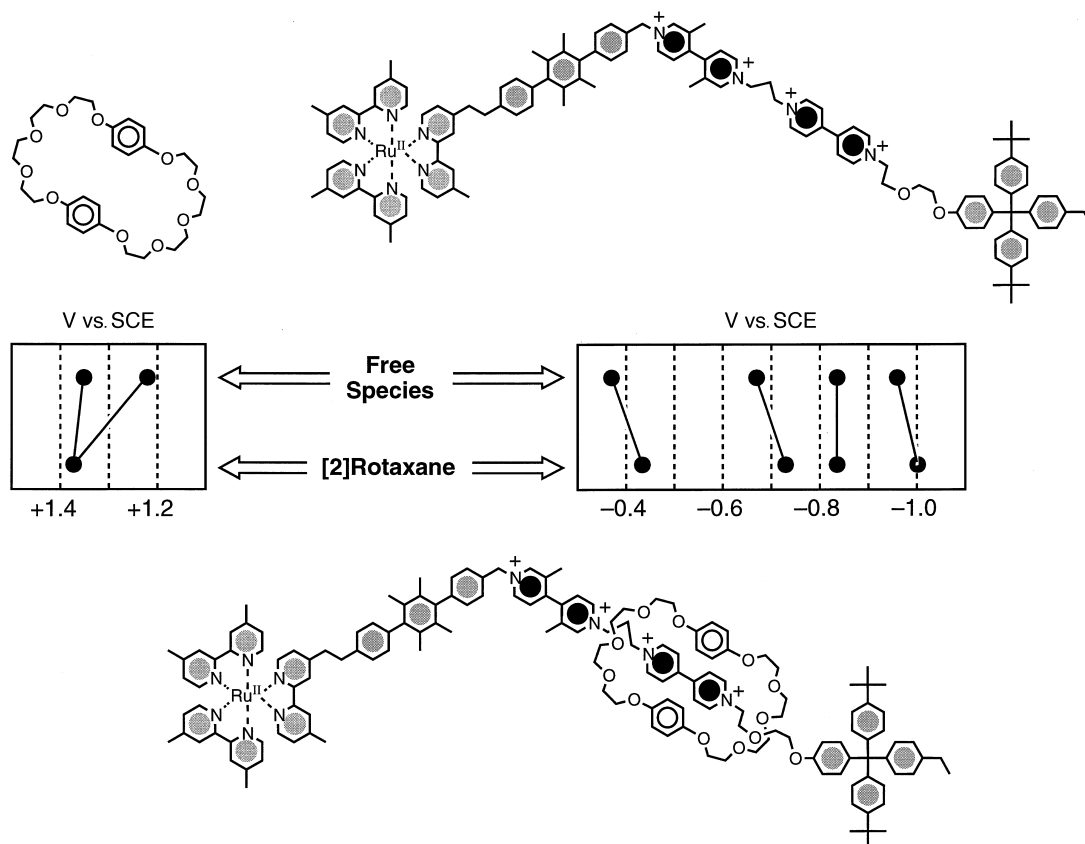

Figure 8. Potential shifts caused by the donor/acceptor interactions between the BPP34C10 ring and dumbbell-shaped components when they are assembled in the [2]rotaxane 1^{6+}.
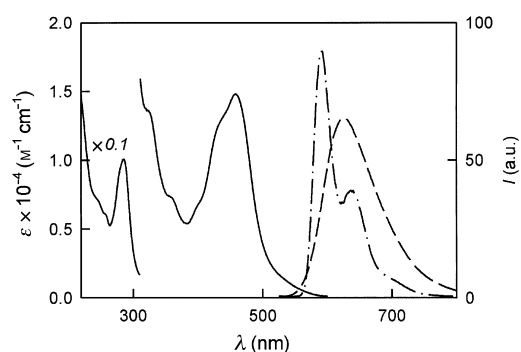
Figure 9. Absorption (MeCN, 298 K, full line) and emission (MeCN, 298 K, dashed line; butyronitrile rigid matrix, 77 K, dotted and dashed line) spectra of a solution of [2]rotaxane 1^{6+}. Excitation was performed at 450 nm.

Table 4. Luminescence and transient absorption data in degassed MeCN solution at 298 K.

		Luminescence of P[a]				Transient absorption decay[b]	
	λ_{max} [nm]	Φ_l[c]	τ [ns]	$k_q \times 10^{-5}$ [s^{-1}][d]	Φ_q[e]	τ [ns]	$k \times 10^{-5}$ [s^{-1}]
3^{2+}	618	0.065 ± 0.005	880 ± 20	–	–	–	–
2^{6+}	618	0.053 ± 0.003	730 ± 10	2.4 ± 0.1	0.18	1200 ± 100	8.3 ± 0.7
1^{6+}	618	0.057 ± 0.003	770 ± 10	1.7 ± 0.1	0.13	4100 ± 100	2.4 ± 0.2

[a] $\lambda_{exc} = 450$ nm. [b] $\lambda_{exc} = 532$ nm, $\lambda_{probe} = 404$ nm. [c] Luminescence quantum yield. [d] Quenching rate constant, calculated by the equation $k_q = 1/\tau - 1/\tau_0$, in which τ_0 is the lifetime of the reference compound 3^{2+}. [e] Yield of the electron transfer quenching process, calculated by the equation $\Phi_q = k_q \times \tau$.

intensity of **P** are quenched (Table 4) in the [2]rotaxane 1^{6+} and in the dumbbell-shaped compound 2^{6+} relative to the values found for the model compound 3^{2+}.[49] The quenching constants k_q, obtained from Equation (1), in which τ_0 is the luminescence lifetime of the reference compound 3^{2+}, are also listed in Table 4.

$$k_q = 1/\tau - 1/\tau_0 \qquad (1)$$

Flash spectroscopy experiments performed on compound 3^{2+} showed (Figure 10) the occurrence of the spectral changes expected for formation of the triplet MLCT excited state of [Ru(bpy)$_3$]$^{2+}$-type compounds.[50] As one can see, an increase in absorption below 400 nm is accompanied by a bleaching

in the spectral region of the ground-state absorption around 450 nm and by an apparent bleaching around 600 nm that arises from the radiative deactivation of the excited state (Figure 9). The transient absorption spectrum was found to decay to the original spectrum with a rate constant in full agreement with the lifetime obtained from luminescence decay. For the purposes of this work, it is particularly important to note the presence of the isosbestic point at 404 nm in the absorption spectra of the ground and excited states of 3^{2+} (Figure 10).

When flash spectroscopy experiments were performed on the [2]rotaxane 1^{6+} or the dumbbell-shaped compound 2^{6+}, an increase in absorbance was observed at 404 nm, instead of the isosbestic point (Figure 11). For both 1^{6+} and 2^{6+}, the risetime of the transient absorption was in agreement, within the experimental error, with the lifetime of the excited state of the component **P**. The transient absorption was found to completely disappear (Figure 11) with rate constant 2.4×10^5 and 8.3×10^5 s^{-1} for 1^{6+} and 2^{6+}, respectively (Table 4). The transient absorption spectrum for 1^{6+} measured 4 μs after the flash showed, besides some residual bleaching in the spectral region of the ground-state absorption of the **P** component, a strong absorption at 400 nm and a weaker one at 600 nm (Figure 12).

Figure 11. Transient absorption kinetics at 404 nm of [2]rotaxane 1^{6+}, dumbbell-shaped component 2^{6+}, and reference compound 3^{2+} as a function of time upon excitation at 532 nm (MeCN, 298 K). The inset shows the complete decay of 1^{6+} on a longer time scale.
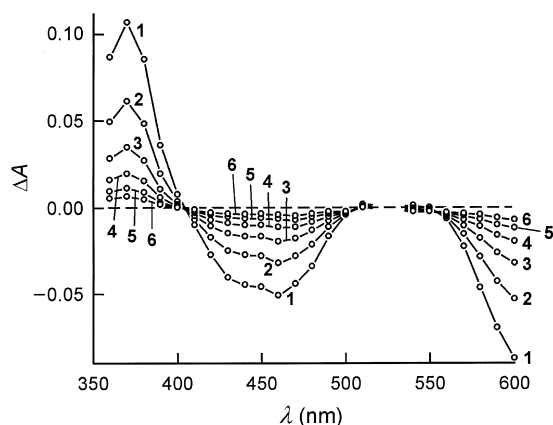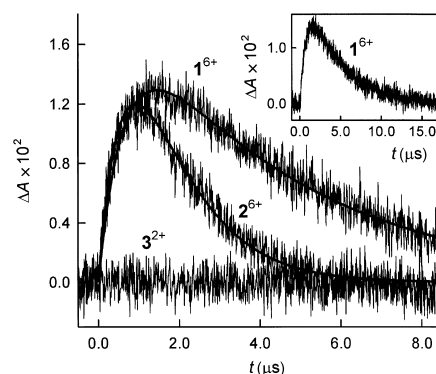

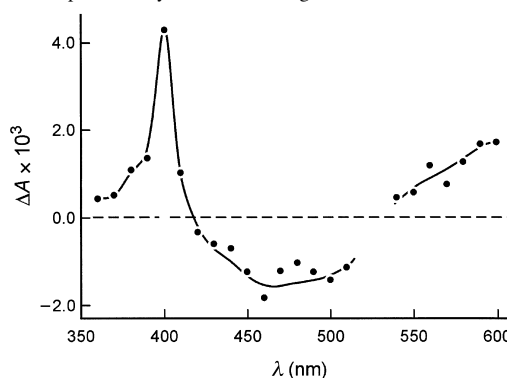Figure 10. Transient absorption difference spectra, obtained in laser flash photolysis (MeCN, 298 K), of reference compound 3^{2+} upon excitation at 532 nm at delay times 0 (**1**), 0.5 (**2**) 1.0 (**3**), 1.5 (**4**), 2.0 (**5**), and 2.5 (**6**) μs after the laser pulse.

Figure 12. Transient absorption difference spectrum of [2]rotaxane 1^{6+} ($\lambda_{exc} = 532$ nm) recorded 4 μs after the laser pulse (MeCN, 298 K).

The transient species formed upon flash excitation of 1^{6+} and 2^{6+} is expected to be[8d, 26, 27] a compound in which an electron has been transferred from the excited state of **P** to one of the two bipyridinium units contained in 1^{6+} and 2^{6+}.[51] In order to understand which of these units was involved in the photoinduced electron transfer process, we recorded the absorption spectra of the one-electron reduced forms of the model compounds 7^{2+} and 8^{2+} in acetonitrile (Figure 13).[52]

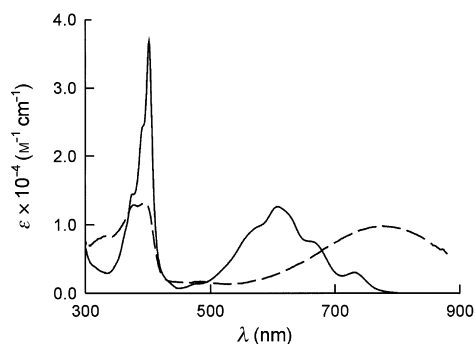Figure 13. Absorption spectra of 7^+ (dashed line) and 8^+ (full line) obtained by photochemical reduction of 7^{2+} and 8^{2+} in degassed MeCN solution at 298 K with [Ru(bpy)$_3$]$^{2+}$ as a photosensitizer and TEOA as a sacrificial electron donor (the absorption spectrum of [Ru(bpy)$_3$]$^{2+}$ has been subtracted).

As one can see, 8^+ shows the well-known,[53] very intense bands with $\lambda_{max} = 397$ and 607 nm, whereas 7^+ shows a weaker and broader absorption band around 400 nm and an absorption band with $\lambda_{max} = 780$ nm.[54] The observed transient spectrum (Figure 12) is clearly very similar to that of 8^+, indicating that, as expected, the photoinduced electron transfer process involves the A_1 station. Whether A_1^- is formed directly or via the intermediate formation of A_2^- followed by a very fast electron transfer from A_2^- to A_1 is a detail that will be discussed below.

When photoexcitation of the [2]rotaxane 1^{6+} or the dumbbell-shaped compound 2^{6+} was performed with a continuous 436 nm light in a degassed MeCN solution containing 0.05 M TEOA, strong spectral changes (see, e.g., Figure 14) were observed. Comparison with the spectra of 7^+ and 8^+ (Figure 13) shows clearly that the photochemical reaction causes a permanent reduction of A_1 to A_1^-. If dioxygen was allowed to enter the irradiated solution, complete disappearance of the characteristic bands of A_1^- was observed, with recovery of the original spectroscopic properties of the [2]rotaxane 1^{6+} and the dumbbell-shaped compound 2^{6+}.
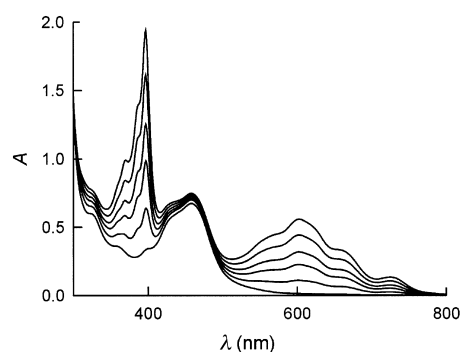

Figure 14. Spectral changes observed upon photoexcitation of the [2]rotaxane 1^{6+} (4.5×10^{-5} M) with 436 nm light in the presence of triethanolamine (0.05 M) in a degassed MeCN solution at 298 K. Irradiation times are 0, 1, 3, 5, 10 and 30 minutes from lower to upper curve. Similar spectral changes were observed in the case of 2^{6+}.

Photochemically driven switching: We will now discuss the results obtained in the light of the two proposed switching mechanisms (Figures 2 and 3).

Intramolecular mechanism: The behavior of the [2]rotaxane 1^{6+} and the dumbbell-shaped compound 2^{6+} can be analyzed on the basis of Figure 15, which shows on an energy scale the processes that take place after photoexcitation of the photoactive component **P**. The energy of the excited state of **P** (2.1 eV) has been obtained from the maximum of the emission band at 77 K (Figure 9). The energies of the various redox states have been obtained from the potential values reported in Table 3. Clearly, the structure of such systems, as far as the photoinduced electron transfer processes are concerned, corresponds to the classical arrangement of triads used in artificial photosynthesis to obtain long-lived charge-separated states.[55] This observation has allowed us to slow the rate of the electronic reset in rotaxane 1^{6+} (Table 4) down to the timescale expected[56] for ring shuttling. We have seen that: i) for both 1^{6+} and 2^{6+}, the rate constant for the quenching of the luminescence of **P** is equal to the rate constant for A_1^-
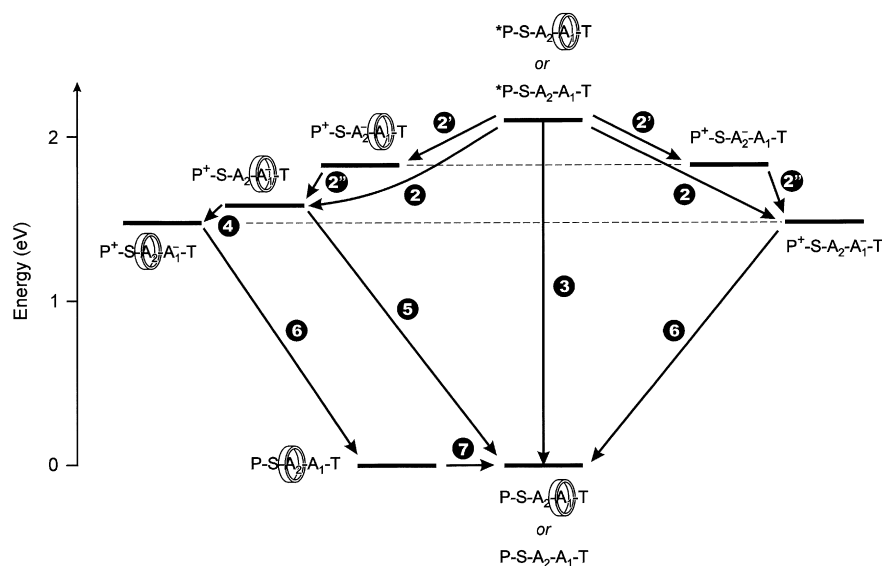

Figure 15. Energy level diagrams for the processes taking place in the [2]rotaxane 1^{6+} (left-hand side) and the dumbbell-shaped compound 2^{6+} (right-hand side) after photoexcitation of the photoactive component **P**. For more details, refer to the text.

formation, ii) the rate constant of the luminescence quenching (or A_1^- formation) is higher in the case of the dumbbell-shaped compound 2^{6+} than for the [2]rotaxane 1^{6+}, iii) the rate constant of the decay of A_1^- is smaller for 1^{6+} than it is for 2^{6+}, and iv) the rate constant for the photoinduced electron transfer (Step 2) is much slower than the rate constant for the intrinsic excited-state decay (Step 3). The result summarized under point i does not allow us to establish whether the reduction of A_1 takes place directly by electron transfer from *P (Step 2 in Figure 15) or through intermediate reduction of A_2, which is more difficult to reduce than A_1, but closer to *P (Step 2′ in Figure 15). The result summarized under point ii, however, rules out the two-step route (Step 2′ followed by Step 2″ in Figure 15), since, in such a case, the quenching rate constants should be equal for 1^{6+} and 2^{6+}. Quenching by direct electron transfer to A_1 is consistent with the larger value of the rate constant in the case of 2^{6+}, just as expected for a more exoergonic reaction in the normal Marcus region (Figure 15). Since the back electron transfer reactions are expected[27, 28] to lie in the Marcus inverted region, the smaller rate constant for the decay of A_1^- in 1^{6+} compared with 2^{6+} (point iii above) suggests that, in the [2]rotaxane, such a reaction is more exoergonic; an observation which means that it takes place when the BPP34C10 ring still encircles A_1^- (Step 5 in Figure 15). Unfortunately, we have not been able to evaluate the rate of Step 4 by electrochemical measurements. Hence, we cannot make a direct comparison between the rates of Steps 4 and 5. Although the above-mentioned indirect evidence would suggest (Figures 2 and 15) that the electronic reset (Step 5) is faster than the BPP34C10 ring displacement (Step 4), we should not be too far from a competition.[56] It should be noted that, in the present system, any further increase in the distance between P and A_1 or in the exergonicity of Step 5, in the attempt to slow down its rate, would compromise the occurrence of the forward (photoinduced) electron transfer Step 2, which is already much slower (point iv above) than the intrinsic decay rate of the excited state, namely, Step 3.

Sacrificial mechanism: We have seen that when photoexcitation of the [2]rotaxane 1^{6+} or the dumbbell-shaped compound 2^{6+} is performed in the presence of a sacrificial electron donor in a degassed MeCN solution, the accumulation of A_1^- is observed (Figure 14). This observation shows (Figure 3b′) that reduction of the oxidized photoactive unit P^+ by the sacrificial donor (Step 8) competes successfully with the back electron transfer reaction (Step 5). Under these conditions, the BPP34C10 ring has all the time it needs to move (Step 4) from A_1^- to A_2, in agreement with the results of the electrochemical experiments. The photoinduced movement of the BPP34C10 ring from the station originally occupied to the other one has therefore been achieved. Electronic reset (Figure 3c′) is obtained when dioxygen, which oxidizes A_1^- to A_1, is allowed to enter the solution (Step 9). As a consequence of this oxidation process, A_1 once again becomes the better π-electron-acceptor station and nuclear reset follows (Step 7 in Figure 3d). Thus, it is clear that the photochemically driven switching of the BPP34C10 ring between stations A_1 and A_2 in the [2]rotaxane 1^{6+} has been achieved by a mechanism involving a sacrificial electron donor.

Conclusion

Calling on a decade's worth of experience, we have taken the design, synthesis, and workings of artificial molecular machines[57] to a considerably higher level of sophistication and performance than has been achieved so far with molecular shuttles.[58] By employing the simplest of thermodynamically controlled self-assembly procedures, namely, slippage,[30] to produce a molecular shuttle from its dumbbell-shaped and ring components, we have constructed a molecular-level system in which the components are capable of undergoing abacus-like movements driven by light inputs. The system we have investigated is a [2]rotaxane, which is comprised of a π-electron-donating macrocycle (BPP34C10) and a dumbbell-shaped component that contains a photoactive stopper and two π-electron-accepting recognition sites (stations), assembled as shown in Schemes 1–4 and Figure 4. We have devised two working schemes for the photoinduced switching of the BPP34C10 ring between stations A_1 and A_2—i) a mechanism based fully on processes which only involves the rotaxane components, that is, an intramolecular mechanism (Figure 2) and ii) a mechanism which requires the help of external reactants, that is, a sacrificial mechanism (Figure 3). The results we have obtained have shown that, although we succeeded in slowing the back electron transfer process (Step 5 in Figure 2) down to the timescale expected for the ring displacement (Step 4), apparently in the present system the latter is still slower than the former. We have clearly shown that the photochemically driven switching can be performed successfully by the sacrificial mechanism (Figure 3). Of course, the intramolecular switching mechanism (Figure 2) is much more appealing than the sacrificial one, principally because the former mechanism implies the conversion of light energy into mechanical energy without generating waste products. In the intramolecular mechanism, the large excess of energy carried by the excited state, compared with that needed for the ring movement, is converted into heat by reversible electron transfer processes. In principle, it would be convenient to use very low-energy excited states. However, they usually exhibit lifetimes that are too short to allow the occurrence of the photoinduced electron transfer process (Step 2 in Figure 2). It should also be noted that, contrary to what happens in the sacrificial mechanism, the intermediate species involved in the intramolecular mechanism need to be stable only for short (submillisecond) time periods. The take-home message is clear. We have sucessfully created a molecular abacus based on a sacrificial electron transfer mechanism. Encouraged by our results, we believe that a molecular abacus based on an intramolecular electron transfer mechanism is within our reach.

Experimental Section

p-phenylene-34-crown-10[59] were synthesized according to literature procedures. Solvents were dried according to literatures procedures.[60] Lithium bromide, ammonium hexafluorophosphate, *n*-butyl lithium, trimethyl borate, palladium (tetrakis)triphenylphosphine, tetrabutylammonium fluoroborate, lithium diisopropylamine, 4,4′-dimethyl-2,2′-bipyridine, bis-*p*-phenylene-34-crown-10 are indicated by the following formulas or acronyms LiBr, NH₄PF₆, *n*BuLi, B(OMe)₃, [Pd(PPh₃)₄], TBAF, LDA, dmbpy, and BPP34C10, respectively. The *tert*-butyldimethylsilyl and *p*-toluenesulfonyl groups are identified by the abbreviations TBDMS and Ts, respectively. Yields refer to chromatographically pure products. Thin-layer chromatography (TLC) was carried out on aluminum sheets coated with silica gel 60 (Merck 5554). Column chromatography was performed on silica gel 60 (Merck, 40–60 nm). Melting points were determined on an Electrothermal 9200 melting point apparatus. Microanalyses were performed by the University of Sheffield Microanalytical Laboratories or by the University of North London Microanalytical Services. Liquid secondary ion mass spectra (LSIMS) were recorded on a VG ZabSpec mass spectrometer equipped with a cesium ion source with *m*-nitrobenzyl alcohol containing a trace of NaOAc. For accurate mass measurements from high-resolution LSIMS (HRLSIMS), the instrument was operated at a resolution of about 6000 by narrow-range voltage scanning along with polyethylene glycol or CsI as reference compounds. Electrospray positive-ion mass spectra (ESMS) were measured on a VG ProSpec triple focusing mass spectrometer with MeCN as mobile phase. Electron impact (EI) mass spectra were recorded at 70 eV on a VG ProSpec mass spectrometer. ¹H NMR spectra were recorded on either a Bruker AC 300 (300 MHz) or a Bruker AMX 400 (400 MHz) or a Bruker DRX 500 (500 MHz) spectrometer. ¹³C NMR spectra were recorded on a Bruker AC 300 (75.5 MHz) or a Bruker AMX 400 (100.6 MHz) or a Bruker DRX 500 (125.8 MHz) spectrometer. The chemical shift values are expressed as δ values and the coupling constant values (J) are in Hertz. The following abbreviations are used for the signal multiplicities or characteristics: s, singlet; d, doublet; dd, doublet of doublets; t, triplet; m, multiplet; q, quartet; quint, quintet; br, broad.

4-(*tert*-Butyldimethylsilyloxymethyl)phenylboronic acid (11): A solution of **10**[31] (12.0 g, 40.0 mmol) in anhydrous THF (80 mL) was cooled down to −78 °C in an atmosphere of dry nitrogen, and a solution of *n*BuLi (1.6 mol L⁻¹ in hexane, 27.5 mL, 44.0 mmol) was added slowly. After stirring the mixture at −78 °C for 1 h, trimethylborate (8.3 g, 80.0 mmol) was added slowly (while maintaining the temperature below −65 °C) and then stirring was continued for a further 1 h at −78 °C. The mixture was allowed to warm up to room temperature and stirred for another 16 h. Hydrochloric acid (5 %, 40 mL) was added to the ice-cooled stirred mixture, which was then extracted several times with Et₂O. The combined organic layers were washed with H₂O and brine, and dried (MgSO₄). Filtration and evaporation of the solvent gave the crude product, which was purified by column chromatography (SiO₂: *n*-hexane/EtOAc, 3:1) to yield the boronic acid **11** (8.4 g, 79 %) as a white solid. M.p. 144 °C; ¹H NMR (300 MHz, CDCl₃, 25 °C): δ = 0.12 (s, 6H), 0.97 (s, 9H), 4.84 (s, 2H), 7.44, 7.47, 8.19, 8.22 (AA′BB′, 4H); ¹³C NMR (75.5 MHz, CDCl₃, 25 °C): δ = −5.2, 18.4, 26.0, 65.0, 125.5, 128.8, 135.7, 146.2; elemental analysis calcd (%) for C₁₃H₂₃BO₃Si: C 58.65, H 8.71; found C 58.88, H 8.65.

4-(4-Bromo-2,3,5,6-tetramethylphenyl)benzyl alcohol (12): An aqueous solution of Na₂CO₃ (2 mol L⁻¹ solution, 10 mL, 20.0 mmol) and the catalyst [Pd(PPh₃)₄] (0.46 g, 5 mol %) were added to a solution of 1,4-dibromo-2,3,5,6-tetramethylbenzene[33] (11.0 g, 37.6 mmol) in PhMe (75 mL). The mixture was purged with nitrogen for 15 min and the boronic acid **11** (2.0 g, 7.52 mmol), dissolved in EtOH (8 mL), was added. The reaction mixture was heated to reflux and stirred for 3 d, during which time it turned black. The mixture was cooled down to room temperature before being diluted with EtOAc (80 mL) and H₂O (80 mL). The aqueous layer was discarded and the organic layer was washed with H₂O and brine, and dried (MgSO₄). Evaporation of solvent in vacuo gave a residue from which an excess of 1,4-dibromo-2,3,5,6-tetramethylbenzene was recovered by crystallization from MeOH. After removal of solvent from the mother liquor, the residue was subjected to desilylation by treating with TBAF (1 mol L⁻¹ solution in THF, 25 mL, 25.0 mmol) in dry THF (75 mL) at room temperature for 12 h. The solvent was removed under reduced pressure, and the crude product was purified by column chromatography (SiO₂: CH₂Cl₂) to yield the alcohol **12** (1.8 g, 75 %), as a white solid. M.p. 112 °C; ¹H NMR (300 MHz, CDCl₃, 25 °C): δ = 1.80 (s, 1H), 1.96 (s, 6H), 2.45 (s, 6H), 4.77 (s, 2H), 7.07, 7.09, 7.41,

7.44 (AA′BB′, 4H); ¹³C NMR (75.5 MHz, CDCl₃, 25 °C): δ = 19.2, 21.2, 65.3, 127.2, 128.4, 129.4, 133.5, 133.8, 139.2, 140.9, 141.6; elemental analysis calcd (%) for C₁₇H₁₉BrO: C 63.96, H 6.00; found C 64.08, H 6.12.

4-(4-Bromo-2,3,5,6-tetramethylphenyl)benzyl bromide (13): A solution of the alcohol **12** (2.3 g, 7.2 mmol) in HBr/AcOH (40 mL, 45 %, w/v) was heated under reflux for 12 h before being cooled down to room temperature and poured into ice-water (200 mL). The mixture was neutralized with 5 % NaHCO₃ and extracted several times with CH₂Cl₂. The combined organic layers were washed with H₂O and brine, and dried (MgSO₄). Removal of the solvent gave the crude product, which was purified by column chromatography (SiO₂: *n*-hexane/CH₂Cl₂, 100:4) to afford the bromide **13** (2.4 g, 89 %) as a white solid. M.p. 116 °C; ¹H NMR (300 MHz, CDCl₃, 25 °C): δ = 1.95 (s, 6H), 2.45 (s, 6H), 4.56 (s, 2H), 7.05, 7.07, 7.43, 7.46 (AA′BB′, 4H); ¹³C NMR (75.5 MHz, CDCl₃, 25 °C): δ = 19.1, 21.1, 33.4, 128.5, 129.2, 129.7, 133.3, 133.9, 136.2, 140.5, 142.4; MS (70 eV, EI): *m/z* (%): 382 (46) [*M*]⁺, 338 (13), 301 (100), 223 (22), 207 (65), 192 (46), 178 (27); elemental analysis calcd (%) for C₁₇H₁₈Br₂: C 53.43, H 4.75; found C 53.53, H 4.78.

4-{2-[4-(4-Bromo-2,3,5,6-tetramethylphenyl)phenyl]ethyl}-4′-methyl-2,2′-bipyridine (14): A solution of 4,4′-dimethyl-2,2′-bipyridine (1.0 g, 5.43 mmol) in dry THF (45 mL) was added dropwise (15 min) at −78 °C, and under a nitrogen atmosphere, to a stirred solution of freshly prepared LDA [from *i*Pr₂NH (0.8 mL, 5.6 mmol) and *n*BuLi (1.6 mol L⁻¹ in hexane, 3.5 mL, 5.6 mmol) in dry THF (10 mL) at −78 °C]; this resulted in a dark brown-red solution. The mixture was allowed to warm up to 0 °C before being stirred further at this temperature for 1 h. A solution of the bromide **13** (2.3 g, 6.0 mmol) in dry THF (15 mL) was added at once, making the reaction mixture light yellow-brown. After 12 h of stirring at room temperature, the orange solution was quenched with MeOH (2 mL) and concentrated in vacuo. The residue was dissolved in CH₂Cl₂, and the resulting solution was washed with H₂O and brine, and dried (MgSO₄). Removal of the solvent gave the crude product, which was subjected to flash column chromatography (SiO₂: CH₂Cl₂/MeOH/NH₄OH, 100:1:0.2) to yield the bipyridine **14** (1.8 g, 66 %) as a white solid. M.p. 172 °C; ¹H NMR (300 MHz, CDCl₃, 25 °C): δ = 1.93 (s, 6H), 2.44 (s, 9H), 3.05 (s, 4H), 6.95, 6.98, 7.19, 7.21 (AA′BB′, 4H), 7.09 (dd, *J* = 5, 2 Hz, 1H), 7.14 (d, *J* = 4 Hz, 1H), 8.24 (d, *J* = 6 Hz, 2H), 8.53 (d, *J* = 5 Hz, 1H), 8.55 (d, *J* = 5 Hz, 1H); ¹³C NMR (75.5 MHz, CDCl₃, 25 °C): δ = 19.1, 21.2, 36.6, 37.5, 121.4, 122.0, 124.1, 127.7, 128.3, 128.6, 129.3, 133.6, 133.7, 139.1, 140.0, 141.1, 148.2, 149.0, 151.6, 156.0, 156.3; MS (70 eV, EI): *m/z* (%): 485 (9) [*M*+H]⁺, 405 (9), 184 (34), 147 (64), 91 (77); elemental analysis calcd (%) for C₂₉H₂₉BrN₂: C 71.75, H 6.02, N 5.77; found C 71.65, H 6.05, N 5.70.

4-{2-[4-(4-Hydroxymethylphenyl)-2,3,5,6-tetramethylphenyl]phenyl}ethyl-4′-methyl-2,2′-bipyridine (15): A mixture of the bromide **14** (1.4 g, 2.9 mmol), the boronic acid **11** (0.91 g, 3.4 mmol), [Pd(PPh₃)₄] (100 mg, 3 mol %), PhMe (20 mL), aqueous Na₂CO₃ solution (3.5 mL, 2 mol L⁻¹, 7.0 mmol), and EtOH (2 mL) was heated under reflux for 2 d. The reaction mixture was then cooled, water (10 mL) was added, and the PhMe layer was separated. The aqueous layer was extracted with EtOAc (2 × 20 mL), the combined organic extracts were dried (MgSO₄) and filtered, and the filtrate evaporated to dryness under reduced pressure. The residue was treated with TBAF (1 mol L⁻¹ solution in THF, 15 mL) at room temperature for 12 h. Solvent was removed in vacuo, and the crude product purified by flash column chromatography (SiO₂: CH₂Cl₂/MeOH/NH₄OH, 100:2:0.35) to afford **15** (0.92g, 62 %) as a white solid. M.p. 194 °C; ¹H NMR (300 MHz, CDCl₃, 25 °C): δ = 1.63 (s, 1H), 1.92 (s, 6H), 1.93 (s, 6H), 2.44 (s, 3H), 3.07 (br s, 4H), 4.77 (d, *J* = 6 Hz, 2H), 7.07, 7.09, 7.43, 7.45 (AA′BB′, 4H), 7.10 (dd, *J* = 5, 2 Hz, 1H), 7.12 (d, *J* = 5 Hz, 1H), 7.17, 7.20, 7.21, 7.24 (AA′BB′, 4H), 8.23 (br s, 1H), 8.27 (br s, 1H), 8.54 (d, *J* = 4 Hz, 1H), 8.56 (d, *J* = 4 Hz, 1H); ¹³C NMR (75.5 MHz, CDCl₃, 25 °C): δ = 18.0, 18.1, 21.2, 36.7, 37.5, 65.3, 121.4, 122.1, 124.1, 124.7, 127.1, 128.4, 129.5, 129.7, 131.8, 132.0, 138.8, 139.0, 140.6, 140.8, 141.1, 142.2, 148.1, 148.2, 149.0, 151.8, 156.0, 156.2; MS (LSIMS): *m/z*: 513.3 [*M*+H]⁺; elemental analysis calcd (%) for C₃₆H₃₆N₂O: C 84.34, H 7.08; found C 84.27, H 7.16, N 5.34.

{Ruthenium(4,4′-dmbpy)₂{4-methyl-4′-{2-{4-[4-(4-hydroxymethylphenyl)-2,3,5,6-tetramethylphenyl]phenyl}ethyl}-2,2′-bipyridine}} bis(hexafluorophosphate) (3·2PF₆): A mixture of [Ru(4,4′-dmbpy)₂]Cl₂[35] (0.99g, 1.83 mmol) and the alcohol **15** (0.85 g, 1.66 mmol) in EtOH/H₂O (60 mL, 3:1, v/v) was heated under reflux and an N₂ atmosphere for 24 h. After removal of the solvent, the residue was purified by flash column chromatography (SiO₂: MeOH/2 mol L⁻¹ NH₄Cl/MeNO₂, 7:2:1). Fractions

containing the product were collected and concentrated in vacuo. The residue was treated with an excess of a 50 % aqueous NH_4PF_6 solution. The red solid was filtered off, washed with H_2O and Et_2O, and dried in vacuo (70 °C/0.1 Torr) to afford the Ru-(hydroxymethyl) complex $\mathbf{3}\cdot 2PF_6$ (1.4 g, 66 %). M.p. 210 °C (decomp); ^1H NMR (300 MHz, CD_3COCD_3, 25 °C): $\delta = 1.78$ (s, 6H), 1.89 (s, 6H), 2.51 – 2.56 (m, 15H), 3.14 (m, 2H), 3.25 (m, 2H), 4.72 (s, 2H), 6.96, 6.99, 7.21, 7.24 (AA′BB′, 4H), 7.09, 7.12, 7.46, 7.49 (AA′BB′, 4H), 7.38 (m, 6H), 7.75 (d, $J = 6$ Hz, 1H), 7.82 (m, 5H), 8.65 (m, 6H); ^{13}C NMR (75 MHz, CD_3COCD_3, 25 °C): $\delta = 18.3$, 21.1, 36.7, 37.6, 64.5, 125.4, 125.8, 127.5, 128.9, 129.3, 129.4, 129.6, 129.9, 130.0, 132.6, 132.7, 133.0, 151.3, 151.5, 132.1, 132.3, 139.3, 141.4, 141.5, 141.6, 141.8, 142.0, 150.8, 154.0, 157.6, 157.7; MS (LSIMS): m/z: 1294 $[M+Na]^+$, 1127 $[M - PF_6]^+$, 981 $[M - 2PF_6]^+$; elemental analysis calcd (%) for $C_{60}H_{60}F_{12}N_6OP_2Ru$: C 56.65, H 4.75, N 6.61; found C 56.75, H 4.75, N 6.46.

{Ruthenium(4,4′-dmbpy)₂{4-methyl-4′-{2-{4-[4-(4-bromomethylphenyl)-2,3,5,6-tetramethylphenyl]phenyl}ethyl]-2,2′-bipyridine}} bis(hexafluorophosphate) (9·2PF₆): A solution of $\mathbf{3}\cdot 2PF_6$ (1.0 g, 0.79 mmol) in HBr/AcOH (12 mL, 45 % w/v) was heated under reflux for 4 h. After cooling, an excess of 50 % aqueous NH_4PF_6 solution was added to precipitate the product, which was then filtered off, washed with H_2O and Et_2O, and dried in vacuo (70 °C/0.1 Torr) to give the Ru-(bromomethyl) complex $\mathbf{9}\cdot 2PF_6$ (0.94 g, 90 %), as an orange solid. M.p. 197 °C (decomp); ^1H NMR (300 MHz, CD_3COCD_3, 25 °C): $\delta = 1.79$ (s, 6H), 1.89 (s, 6H), 2.51 – 2.56 (m, 15H), 3.14 (m, 2H), 3.25 (m, 2H), 4.76 (m, 2H), 6.97, 6.99, 7.22, 7.24 (AA′BB′, 4H), 7.15, 7.17, 7.58, 7.60 (AA′BB′, 4H), 7.38 (m, 6H), 7.75 (d, $J = 6$ Hz, 1H), 7.82 – 7.84 (m, 5H), 8.66 (m, 6H); ^{13}C NMR (125 MHz, CD_3COCD_3, 25 °C): $\delta = 18.2$, 21.1, 34.4, 36.7, 37.6, 125.5, 125.9, 128.9, 129.3, 129.5, 129.6, 130.1, 130.2, 130.6, 132.6, 132.7, 132.8, 151.4, 151.6, 132.2, 132.3, 137.5, 139.3, 141.4, 141.4, 141.9, 143.8, 150.9, 154.1, 157.7, 157.8; MS (LSIMS): m/z: 1189 $[M - PF_6]^+$, 1045 $[M - 2PF_6]^+$; elemental analysis calcd (%) for $C_{60}H_{59}BrF_{12}N_6P_2Ru$: C 53.98, H 4.45, N 6.29; found C 54.04, H 4.37, N 6.26.

N-{2-{4-[4-Ethylphenyl-bis(4-tert-butylphenyl)methyl]phenoxy}ethoxyethyl]-4,4′-bipyridinium Hexafluorophosphate (17·PF₆): A mixture of $\mathbf{16}^{[36]}$ (4.45 g, 6.2 mmol), 4,4′-bipyridine (5.8 g, 37.2 mmol) and anhydrous LiBr (0.2 g) in dry MeCN (30 mL) was heated under reflux for 3 d. The solvent was evaporated to dryness and the crude product was purified by column chromatography (SiO_2, the first eluent was MeOH to remove an excess of 4,4′-bipyridine and the second eluent MeOH/$MeNO_2$/2 mol L^{-1} NH_4Cl, 8:1.9:0.1). The isolated residue was dissolved in H_2O/Me_2CO, and a saturated aqueous solution of NH_4PF_6 was added. After the evaporation of the a Me_2CO, the precipitated solid was filtered off, washed with H_2O, and dried (70 °C/0.1 Torr) to yield $\mathbf{17}\cdot PF_6$ (4.3g, 82 %). M.p. 182 °C; ^1H NMR (300 MHz, CD_3CN, 25 °C): $\delta = 1.17$ (t, $J = 8$ Hz, 3H), 1.26 (s, 18H), 2.58 (q, $J = 8$ Hz, 2H), 3.77 (m, 2H), 4.00 (m, 4H), 4.70 (m, 2H), 6.71 (d, $J = 9$ Hz, 2H), 7.07 – 7.12 (m, 10H), 7.29 (d, $J = 8$ Hz, 4H), 7.83 (d, $J = 6$ Hz, 2H), 8.19 (d, $J = 7$ Hz, 2H), 8.72 – 8.86 (m, 4H); ^{13}C NMR (75.5 MHz, CD_3CN, 25 °C): $\delta = 15.9$, 28.8, 31.6, 34.9, 62.4, 64.1, 68.1, 69.7, 70.4, 114.3, 125.4, 126.6, 128.0, 131.3, 131.6, 132.7, 140.8, 142.7, 143.1, 145.5, 145.8, 146.5, 149.5, 151.4, 154.8, 157.5; elemental analysis calcd (%) for $C_{49}H_{55}F_6N_2O_2P$: C 69.33, H 6.53, N 3.30; found C 69.16, H 6.71, N 3.27.

N-(3-Bromopropyl)-N′-{2-{4-[4-ethylphenyl-bis(4-tert-butylphenyl)methyl]phenoxy}ethoxy}ethyl-4,4′-bipyridinium bis(hexafluorophosphate) (18·2PF₆): A solution of $\mathbf{17}\cdot PF_6$ (2.54 g, 3.0 mmol) and 1,3-dibromopropane (6.1 g, 30.0 mmol) in dry MeCN (40 mL) was heated under reflux for 4 d under nitrogen atmosphere. The solvent was removed under reduced pressure and the residue was purified by column chromatography (SiO_2: MeOH/$MeNO_2$/2 mol L^{-1} NH_4Cl, 8:1.9:0.1) to afford, after counterion exchange [H_2O/Me_2CO, a saturated aqueous solution of NH_4PF_6], $\mathbf{18}\cdot 2PF_6$ (2.3 g, 69 %) as a white-gray solid. M.p. 212 °C (decomp); ^1H NMR (300 MHz, CD_3COCD_3, 25 °C): $\delta = 1.18$ (t, $J = 8$ Hz, 3H), 1.28 (s, 18H), 2.59 (q, $J = 8$ Hz, 2H), 2.77 (quint, $J = 7$ Hz, 2H), 3.65 (t, $J = 7$ Hz, 2H), 3.88 (m, 2H), 4.10 (m, 2H), 4.23 (m, 2H), 5.06 – 5.16 (m, 4H), 6.81 (d, $J = 7$ Hz, 2H), 7.05 – 7.13 (m, 10H), 7.30 (d, $J = 8$ Hz, 4H), 8.77 (d, $J = 7$ Hz, 2H), 8.81 (d, $J = 6$ Hz, 2H), 9.38 (d, $J = 7$ Hz, 2H), 9.43 (d, $J = 6$ Hz, 2H); ^{13}C NMR (75.5 MHz, $CDCl_3$, 25 °C): $\delta = 15.9$, 28.7, 29.7, 31.5, 34.0, 34.9, 61.3, 62.5, 64.1, 68.0, 69.7, 70.4, 114.4, 125.7, 127.7, 128.0, 128.3, 131.2, 131.5, 132.7, 141.0, 142.8, 145.5, 145.8, 146.8, 147.2, 149.6, 151.0, 157.4; elemental analysis calcd (%) for $C_{52}H_{61}BrF_{12}N_2O_2P_2$: C 55.97, H 5.51, N 2.51; found C 56.11, H 5.59, N 2.36.

N-[3-(3,3′-Dimethyl-4,4′-bipyridinium-1-yl)propyl]-N′-{2-{4-[4-ethylphenyl-bis(4-tert-butylphenyl)methyl]phenoxy}ethoxy}ethyl-4,4′-bipyridinium tris(hexafluorophosphate) (19·3PF₆): A solution of $\mathbf{18}\cdot 2PF_6$ (1.5 g,

1.34 mmol) and 3,3′-dimethyl-4,4′-bipyridine$^{[37]}$ (2.4 g, 13.4 mmol) in dry MeCN (30 mL) was heated under reflux for 7 d. After removal of solvent by evaporation, the residue was purified by column chromatography (SiO_2: MeOH/2 mol L^{-1} $NH_4Cl/MeNO_2$, 7:2:1) to afford, after counterion exchange (50 % aqueous solution NH_4PF_6), $\mathbf{19}\cdot 3PF_6$ (1.7 g, 93 %) as a light brown solid. M.p. 218 °C (decomp); ^1H NMR (300 MHz, CD_3CN, 25 °C): $\delta = 1.18$ (t, $J = 8$ Hz, 3H), 1.27 (s, 18H), 2.23 (s, 3H), 2.25 (s, 3H), 2.59 (q, $J = 7$ Hz, 2H), 2.76 (quint, $J = 8$ Hz, 2H), 3.80 (m, 2H), 4.00 – 4.11 (m, 4H), 4.67 – 4.84 (m, 6H), 6.82 (d, $J = 9$ Hz, 2H), 7.09 – 7.20 (m, 10H), 7.31 (d, $J = 8$ Hz, 4H), 7.77 (br s, 1H), 7.87 (d, $J = 6$ Hz, 1H), 8.36 (d, $J = 7$ Hz, 2H), 8.45 (d, $J = 7$ Hz, 2H), 8.69 (d, $J = 6$ Hz, 2H), 8.76 (br s, 2H), 8.91 (d, $J = 7$ Hz, 2H), 8.94 (d, $J = 7$ Hz, 2H); ^{13}C NMR (75.5 MHz, CD_3CN, 25 °C): $\delta = 15.9$, 16.8, 17.4, 28.8, 31.6, 32.8, 34.9, 58.7, 59.3, 62.7, 64.1, 68.0, 69.7, 70.5, 114.4, 125.5, 127.8, 128.0, 128.6, 129.0, 131.2, 131.5, 132.8, 139.2, 140.9, 142.7, 143.1, 145.5, 145.8, 146.0, 146.5, 146.6, 146.9, 147.2, 149.5, 150.0, 151.0, 151.3, 156.2, 157.5; MS (LSIMS): m/z: 1220 $[M - PF_6]^+$, 1075 $[M - 2PF_6]^+$, 929 $[M - 3PF_6]^+$; elemental analysis calcd (%) for $C_{64}H_{73}F_{18}N_4O_2P_3$: C 56.31, H 5.39, N 4.10; found C 56.38, H 5.39, N 3.96.

N-{3-[(1′-Benzyl)-3,3′-dimethyl-4,4′-bipyridinium-1-yl]propyl}-N′-{2-{4-[4-ethylphenyl-bis(4-tert-butylphenyl)methyl]phenoxy}ethoxy}ethyl-4,4′-bipyridinium tetrakis(hexafluorophosphate) (4·4PF₆): A solution of $\mathbf{19}\cdot 3PF_6$ (158 mg, 0.116 mmol) and benzyl bromide (200 mg, 1.17 mmol) in dry MeCN (10 mL) was heated under reflux for 4 d. Solvent was removed on a rotary evaporator, and the residue was subjected to flash column chromatography (SiO_2: MeOH/2 mol L^{-1} $NH_4Cl/MeNO_2$, 7:2:1) to afford, after counterion exchange (50 % aqueous solution NH_4PF_6), the quaternary salt $\mathbf{4}\cdot 4PF_6$ (140 mg, 75 %). M.p. 238 °C (decomp); ^1H NMR (500 MHz, CD_3COCD_3, 25 °C): $\delta = 1.20$ (t, $J = 8$ Hz, 3H), 1.29 (s, 18H), 2.37 (s, 3H), 2.41 (s, 3H), 2.60 (q, $J = 7$ Hz, 2H), 3.13 (quint, $J = 8$ Hz, 2H), 3.90 (m, 2H), 4.13 (m, 2H), 4.26 (m, 2H), 5.11 (t, $J = 7$ Hz, 2H), 5.16 (t, $J = 5$ Hz, 2H), 5.19 (t, $J = 7$ Hz, 2H), 6.08 (s, 2H), 6.83 (d, $J = 9$ Hz, 2H), 7.08 – 7.13 (m, 10H), 7.31 (d, $J = 9$ Hz, 4H), 7.48 – 7.52 (m, 3H), 7.65 – 7.68 (m, 2H), 8.18 (d, $J = 6$ Hz, 1H), 8.20 (d, $J = 6$ Hz, 1H), 8.79 (d, $J = 7$ Hz, 2H), 8.81 (d, $J = 7$ Hz, 2H), 9.12 (d, $J = 6$ Hz, 1H), 9.20 (br s, 1H), 9.26 (d, $J = 6$ Hz, 1H), 9.35 (d, $J = 7$ Hz, 2H), 9.39 (br s, 1H), 9.41 (d, $J = 7$ Hz, 2H); ^{13}C NMR (125 MHz, CD_3COCD_3, 25 °C): $\delta = 14.9$, 16.3, 16.4, 30.7, 32.1, 34.6, 58.6, 58.8, 61.9, 64.8, 67.1, 69.0, 69.6, 113.2, 124.2, 126.8, 126.8, 126.9, 127.6, 127.8, 127.9, 129.3, 129.5, 129.9, 130.5, 130.8, 132.0, 142.7, 142.8, 146.1, 146.4, 146.6, 32.1, 33.9, 133.2, 138.1, 138.2, 139.7, 141.5, 144.3, 144.7, 148.3, 150.3, 150.6, 152.3, 156.7; MS (LSIMS): m/z: 1456 $[M - PF_6]^+$, 1311 $[M - 2PF_6]^+$, 1165 $[M - 3PF_6]^+$; elemental analysis calcd (%) for $C_{71}H_{80}F_{24}N_4O_2P_4$: C 53.23, H 5.04, N 3.50; found C 53.19, H 5.11, N 3.52.

Dumbbell-shaped compound 2·6PF₆: A mixture of $\mathbf{9}\cdot 2PF_6$ (0.80 g, 0.6 mmol) and $\mathbf{19}\cdot 3PF_6$ (0.82 g, 0.6 mmol) in dry MeCN (40 mL) was heated under reflux in an N_2 atmosphere for 6 d. After cooling, the solvent was evaporated and the residue was purified by flash column chromatography (SiO_2: MeOH/2 mol L^{-1} $NH_4Cl/MeNO_2$, 7:2:1). The fractions containing the product were combined and concentrated in vacuo, and the residue was then treated with an excess of a 50 % aqueous NH_4PF_6 solution. The red solid was filtered off, washed with H_2O and diethyl ether, and dried in vacuo (80 °C/0.1 Torr) to afford the dumbbell-shaped compound $\mathbf{2}\cdot 6PF_6$ (1.05 g, 63 %). M.p .216 °C (decomp); ^1H NMR (500 MHz, CD_3COCD_3, 31 °C): $\delta = 1.19$ (t, $J = 8$ Hz, 3H), 1.29 (s, 18H), 1.79 (s, 6H), 1.88 (s, 6H), 2.40 (s, 3H), 2.44 (s, 3H), 2.50 (s, 3H), 2.52 (s, 3H), 2.56 – 2.58 (m, 9H), 2.60 (q, $J = 8$ Hz, 2H), 3.07 – 3.18 (m, 4H), 3.19 – 3.29 (m, 2H), 3.90 (m, 2H), 4.13 (m, 2H), 4.26 (m, 2H), 5.13 (t, $J = 8$ Hz, 2H), 5.16 (t, $J = 5$ Hz, 2H), 5.20 (t, $J = 8$ Hz, 2H), 6.17 (s, 2H), 6.83 (d, $J = 9$ Hz, 2H), 6.97 (d, $J = 8$ Hz, 2H), 7.09 – 7.14 (m, 10H), 7.24 (d, $J = 8$ Hz, 2H), 7.28 – 7.31 (m, 6H), 7.32 – 7.37 (m, 6H), 7.73 (d, $J = 6$ Hz, 2H), 7.76 – 7.82 (m, 6H), 8.21 (d, $J = 6$ Hz, 1H), 8.23 (d, $J = 6$ Hz, 1H), 8.60 – 8.62 (m, 6H), 8.79 (d, $J = 7$ Hz, 2H), 8.82 (d, $J = 7$ Hz, 2H), 9.14 (d, $J = 7$ Hz, 1H), 9.23 (s, 1H), 9.31 (d, $J = 7$ Hz, 1H), 9.37 (d, $J = 7$ Hz, 2H), 9.40 (d, $J = 7$ Hz, 2H), 9.47 (s, 1H); ^{13}C NMR (125 MHz, CD_3COCD_3, 25 °C): $\delta = 15.8$, 17.2, 17.3, 18.2, 18.3, 21.0, 21.1, 31.6, 31.6, 33.0, 34.8, 36.7, 37.6, 59.5, 59.7, 62.8, 65.5, 68.0, 69.9, 70.5, 114.1, 125.1, 125.4, 125.8, 127.7, 127.8, 128.5, 128.8, 128.9, 129.3, 129.6, 130.1, 130.3, 131.4, 131.7, 132.8, 143.7, 147.0, 147.3, 147.5, 151.4, 151.6, 151.7, 132.1, 132.3, 132.4, 139.0, 139.1, 139.4, 140.6, 141.0, 141.4, 142.1, 142.4, 145.2, 145.4, 145.6, 149.2, 150.9, 151.2, 153.2, 154.2, 157.6, 157.7, 157.8; MS (LSIMS): m/z: 2620 $[M - PF_6]^+$, 2475 $[M - 2PF_6]^+$, 2330 $[M - 3PF_6]^+$, 2185 $[M - 4PF_6]^+$; elemental analysis calcd (%) for $C_{124}H_{132}F_{36}N_{10}O_2P_6Ru$: C 53.86, H 4.81, N 5.07; found C 53.46, H 4.51, N 4.91.

[2]Rotaxane 1·6PF₆: A solution of the dumbbell-shaped compound **2·6PF₆** (280 mg, 0.1 mmol) and bis-*p*-phenylene-34-crown-10 (268 mg, 0.5 mmol) in dry MeCN (3 mL) was stirred at 50 °C for 4 d. The solvent was removed in vacuo and the residue was purified by flash column chromatography (SiO₂: MeOH/2 mol L⁻¹ NH₄Cl/MeNO₂, 7:2:1) to give, after counterion exchange (50 % aqueous solution NH₄PF₆) the dumbbell compound **2·6PF₆** (80 mg) and the rotaxane **1·6PF₆** (140 mg, 59 % based on the amount of the reacted dumbbell) as a red solid. M.p. 193 °C (decomp); ¹H NMR (400 MHz, CD₃COCD₃, 31 °C): $\delta = 1.19$ (t, $J = 8$ Hz, 3H), 1.28 (s, 18H), 1.79 (s, 6H), 1.88 (s, 6H), 2.44 (s, 3H), 2.47 (s, 3H), 2.50 (s, 3H), 2.52 (s, 3H), 2.53–2.56 (m, 9H), 2.59 (q, $J = 8$ Hz, 2H), 3.07–3.15 (m, 2H), 3.18–3.29 (m, 4H), 3.60–3.66 (m, 8H), 3.68–3.74 (m, 8H), 3.76–3.81 (m, 8H), 3.82–3.87 (m, 8H), 4.04 (m, 2H), 4.24 (m, 2H), 4.34 (m, 2H), 5.13–5.22 (m, 6H), 6.18 (s, 2H), 6.25 (s, 8H), 6.88 (d, $J = 9$ Hz, 2H), 6.97 (d, $J = 8$ Hz, 2H), 7.08–7.10 (m, 10H), 7.24 (d, $J = 8$ Hz, 2H), 7.27 (d, $J = 9$ Hz, 2H), 7.29–7.36 (m, 10H), 7.73 (d, $J = 6$ Hz, 2H), 7.76–7.82 (m, 6H), 8.21 (d, $J = 6$ Hz, 1H), 8.27 (d, $J = 6$ Hz, 1H), 8.31 (d, $J = 7$ Hz, 4H), 8.61–8.63 (m, 6H), 9.14 (d, $J = 5$ Hz, 2H), 9.16 (d, $J = 6$ Hz, 2H), 9.21 (d, $J = 6$ Hz, 1H), 9.29 (s, 1H), 9.32 (d, $J = 6$ Hz, 1H), 9.48 (s, 1H); ¹³C NMR (100 MHz, CD₃COCD₃, 25 °C): $\delta = 15.8, 17.4, 21.1, 31.6, 32.6, 36.7, 37.6, 59.0, 59.9, 62.1, 65.5, 68. 2. 68.5, 69.5, 70.4, 70.8, 71.2, 71.5, 114.1, 115.8, 125.1, 125.5, 125.9, 126.3, 127.6, 128.8, 129.3, 129.6, 130.1, 130.3, 131.4, 131.7, 132.9, 143.8, 146.7, 147.2, 147.3, 151.4, 151.6, 132.1, 132.3, 132.4, 139.2, 139.4, 140.6, 141.0, 141.4, 142.1, 142.4, 145.2, 145,4, 145.6, 147.8, 149.2, 150.9, 153.2, 154.2 157.8$; MS (LSIMS): m/z: 3303 $[M]^+$, 3157 $[M − PF_6]^+$, 3012 $[M − 2PF_6]^+$, 2867 $[M − 3PF_6]^+$; ESMS: m/z: 1506 $[M − 2PF_6]^{2+}$, 956 $[M − 3PF_6]^{3+}$, 680 $[M − 4PF_6]^{4+}$; elemental analysis calcd (%) for $C_{152}H_{172}F_{36}N_{10}O_{12}P_6Ru$: C 55.29, H 5.25, N 4.24; found C 55.13, H 5.15, N 4.13.

Photophysical and photochemical experiments: Measurements were carried out at 298 K on MeCN (Merck Uvasol) solutions with concentrations ranging from 5×10^{-6} to 1×10^{-4} M. UV-Vis absorption spectra were recorded on air-equilibrated solutions with a Perkin Elmer λ16 spectrophotometer. Uncorrected luminescence spectra were obtained with a Perkin Elmer LS-50 spectrofluorimeter, equipped with a Hamamatsu R928 phototube, on solutions degassed with at least four freeze-pump-thaw cycles and sealed under vacuum ($p = 7 \times 10^{-9}$ atm). Luminescence quantum yields were determined by the optically dilute method[61] with $[Ru(bpy)_3]^{2+}$ in air equilibrated water ($\Phi = 0.028$)[62] as a standard. Low-temperature (77 K) luminescence spectra were obtained on a butyronitrile (Fluka) rigid matrix. Photochemical experiments were carried out by irradiation of degassed solutions (see above) with a tungsten halogen lamp (150 W, $\lambda > 350$ nm). Luminescence lifetimes were measured by time-correlated single-photon counting with Edinburgh Instruments DS199 equipment. The exciting light ($\lambda = 300$ nm) was produced by a gas arc lamp (model nF900, filled with D₂) that delivered pulses of about 1 ns (fwhm). The detector was a cooled Hamamatsu R928 photomultiplier. Nanosecond transient absorption experiments were performed by exciting the sample with 10 ns (fwhm) pulses of a Continuum Surelite I-10 Nd:Yag laser (10 Hz repetition rate) and using a pulsed 150 W Xe lamp, perpendicular to the laser beam, as a probing light. Excitation was performed at $\lambda = 532$ nm (obtained by frequency doubling) with a laser power of 1.5 mJ per pulse, except for the kinetic studies carried out at $\lambda_{probe} = 404$ nm (see text), in which the laser power was 4 mJ per pulse. The Xe lamp was equipped with an Applied Photophysics power supply (Model 40) and pulsing unit (Model 410, 2 ms pulses). A shutter (Oriel 71445), placed between the lamp and the sample, was opened for 100 ms to prevent phototube fatigue and photodecomposition. Suitable pre- and post-cutoff, and bandpass filters were also used to avoid photodecomposition and interferences from scattered light. The light was collected in an LDC Analytical monochromator, detected by a Hamamatsu R928 tube, and recorded on a LeCroy 9360 (600 MHz) oscilloscope. Synchronous timing of the system was achieved by means of a built-in-house digital logic circuit. The absorption transient decays were plotted as $\Delta A = \log(I_0/I_t)$ vs. time, where I_0 and I_t were the probing light intensity prior to the laser pulse and after delay t, respectively. Each decay was obtained by averaging ten pulses. Transient absorption spectra were obtained from the decays measured at various wavelengths, by sampling the absorbance changes at constant delay time. The same laser/monochromator/phototube setup was employed to measure luminescence lifetimes, giving the same values (within 2 %) obtained by single-photon counting. Lifetimes were also checked by a Spex Fluorolog-τ3 system, which uses the phase-modulation technique (exciting light modulated in the 0.1–10 MHz range; $\lambda_{exc} = 450$ nm). The frequency-domain intensity decays (phase-angle and modulation vs. frequency) were analyzed with the DataMax software.

Electrochemical measurements: Conventional electrochemical experiments were carried out in argon-purged MeCN solution at room temperature with a Princeton Applied Research 273 multipurpose instrument interfaced to a personal computer. In the cyclic voltammetry (CV) and differential pulse voltammetry (DPV) experiments, the working electrode was a glassy carbon electrode (0.08 cm², Amel); its surface was routinely polished with a 0.05 μm alumina-water slurry on a felt surface, immediately prior to use. In all cases, the counter electrode was a Pt wire and the reference was a saturated calomel electrode (SCE) separated with a fine glass frit. The concentration of the compounds examined was 5.0×10^{-4} M; tetraethylammonium hexafluorophosphate (0.05 M) was added as the supporting electrolyte. Cyclic voltammograms were obtained as sweep rates of 20, 50, 200, 500, and 1000 mV s⁻¹; DPV experiments were performed with a scan rate of 20 mV s⁻¹, a pulse height of 75 mV, and a duration of 40 ms. Ferrocene was present as an internal standard. The experimental error was estimated to be ±10 mV. Attempts were made to study the electrochemical behavior of the [2]rotaxane **1**⁶⁺ by using very fast scan rates (up to 3×10^6 V s⁻¹) with a CH Instruments Model 660 Electrochemical Workstation.[45] Unfortunately, severe adsorption phenomena on both Pt and glassy carbon microelectrodes prevented the acquisition of meaningful results.

Acknowledgements

[1] a) D. S. Goodsell, *Our Molecular Nature: The Body's Motors, Machines, and Messages*, Copernicus, New York, **1996**; b) P. D. Boyer, *Ann. Rev. Biochem.* **1997**, *66*, 717–749; c) P. R. Cook, *Science* **1999**, *284*, 1790–1795.

[2] R. P. Feynman, *Eng. Sci.* **1960**, *23*, 22–36.

[3] S. Shinkai, O. Manabe, *Top. Curr. Chem.* **1984**, *121*, 67–104.

[4] a) J.-M. Lehn, *Supramolecular Chemistry: Concepts and Perspectives*, VCH, Weinheim, **1995**; b) *Comprehensive Supramolecular Chemistry*, *Vol. 1–10* (Eds.: J.-M. Lehn, J. L. Atwood, J. E. D. Davies, D. D. MacNicol, F. Vögtle), Pergamon, Oxford, **1996**.

[5] For reviews on molecular-level machines, see: a) K. Mislow, *Chemtracts: Org. Chem.* **1989**, *2*, 151–174; b) A. P. de Silva, C. P. McCoy, *Chem. Ind.* **1994**, 992–996; c) A. C. Benniston, *Chem. Soc. Rev.* **1996**, *25*, 427–436; d) M. D. Ward, *Chem. Ind.* **1997**, 640–645; e) V. Balzani, M. Gómez-López, J. F. Stoddart, *Acc. Chem. Res.* **1998**, *31*, 405–414; f) J.-P. Sauvage, *Acc. Chem. Res.* **1998**, *31*, 611–619; g) P. L. Boulas, M. Gomez-Kaifer, L. Echegoyen, *Angew. Chem.* **1998**, *110*, 226–258; *Angew. Chem. Int. Ed.* **1998**, *37*, 216–247; h) D. A. Leigh, A. Murphy, *Chem. Ind.* **1999**, 178–183; i) L. Fabbrizzi, M. Licchelli, P. Pallavicini, *Acc. Chem. Res.* **1999**, *32*, 846–853; j) P. Piotrowiak, *Chem. Soc. Rev.* **1999**, *28*, 143–150; k) M.-J. Blanco, M. C. Jiménez, J.-C. Chambron, V. Heitz, M. Linke, J.-P. Sauvage, *Chem. Soc. Rev.* **1999**, *28*, 293–305; l) *Molecular Switches* (Ed.: B. L. Feringa), Wiley-VCH, Weinheim, **2000**; m) A. E. Kaifer, *Acc. Chem. Res.* **1999**, *32*, 62; n) M. D. Ward, *Chem. Ind.* **2000**, 22–26; o) Z. Asfari, J. Vicens, *Actual. Chim.* **2000**, *March*, 5–11.

[6] For accounts, books, and reviews on mechanically-interlocked molecules and supermolecules, see: a) G. Schill, *Catenanes, Rotaxanes and Knots*, Academic Press, New York, **1971**; b) D. M. Walba, *Tetrahedron* **1985**, *41*, 3161–3212; c) C. O. Dietrich-Buchecker, J.-P. Sauvage, *Chem. Rev.* **1987**, *87*, 795–810; d) C. O. Dietrich-Buchecker, J.-P. Sauvage, *Bioorg. Chem. Front.* **1991**, *2*, 195–248; e) H. W. Gibson, H.

Marand, *Adv. Mater.* **1993**, *5*, 11–21; f) J.-C. Chambron, C. O. Dietrich-Buchecker, J.-P. Sauvage, *Top. Curr. Chem.* **1993**, *165*, 131–162; g) H. W. Gibson, M. C. Bheda, P. T. Engen, *Prog. Polym. Sci.* **1994**, *19*, 843–945; h) D. B. Amabilino, J. F. Stoddart, *Chem. Rev.* **1995**, *95*, 2725–2828; i) M. Belohradsky, F. M. Raymo, J. F. Stoddart, *Collect. Czech. Chem. Commun.* **1996**, *61*, 1–43; j) M. Fujita, K. Ogura, *Coord. Chem. Rev.* **1996**, *148*, 249–264; k) R. Jäger, F. Vögtle, *Angew. Chem.* **1997**, *109*, 966–980; *Angew. Chem. Int. Ed.* **1997**, *36*, 930–944; l) M. Belohradsky, F. M. Raymo, J. F. Stoddart, *Collect. Czech. Chem. Commun.* **1997**, *62*, 527–557; m) S. A. Nepogodiev, J. F. Stoddart, *Chem. Rev.* **1998**, *98*, 1959–1976; n) M. Fujita, *Acc. Chem. Res.* **1999**, *32*, 53–61; o) F. M. Raymo, J. F. Stoddart, *Chem. Rev.* **1999**, *99*, 1643–1664; p) *Molecular Catenanes, Rotaxanes and Knots* (Eds.: J.-P. Sauvage, C. O. Dietrich-Buchecker), VCH-Wiley, Weinheim, **1999**; q) G. A. Breault, C. A. Hunter, P. C. Mayers, *Tetrahedron*, **1999**, *55*, 5265–5293.

[7] V. Balzani, F. Scandola, *Supramolecular Photochemistry*, Horwood, Chichester, **1991**.

[8] a) R. Ballardini, V. Balzani, M. T. Gandolfi, L. Prodi, M. Venturi, D. Philp, H. G. Ricketts, J. F. Stoddart, *Angew. Chem.* **1993**, *105*, 1362–1364; *Angew. Chem. Int. Ed. Engl.* **1993**, *32*, 1301–1303; b) P. R. Ashton, R. Ballardini, V. Balzani, S. E. Boyd, A. Credi, M. T. Gandolfi, M. Gómez-López, S. Iqbal, D. Philp, J. A. Preece, L. Prodi, H. G. Ricketts, J. F. Stoddart, M. S. Tolley, M. Venturi, A. J. P. White, D. J. Williams, *Chem. Eur. J.* **1997**, *3*, 152–170; c) P. R. Ashton, V. Balzani, O. Kocian, L. Prodi, N. Spencer, J. F. Stoddart, *J. Am. Chem. Soc.* **1998**, *120*, 11190–11191; d) P. R. Ashton, R. Ballardini, V. Balzani, E. C. Constable, A. Credi, O. Kocian, S. J. Langford, J. A. Preece, L. Prodi, E. R. Schofield, N. Spencer, J. F. Stoddart, S. Wenger, *Chem. Eur. J.* **1998**, *4*, 2413–2422.

[9] R. Arad-Yelling, B. S. Green, *Nature* **1994**, *371*, 320–322.

[10] M. Bauer, W. M. Müller, K. Rissanen, F. Vögtle, *Liebigs Ann.* **1995**, 649–656.

[11] A. C. Benniston, A. Harriman, V. M. Lynch, *J. Am. Chem. Soc.* **1995**, *117*, 5275–5291.

[12] a) A. Livoreil, J.-P. Sauvage, N. Armaroli, V. Balzani, L. Flamigni, B. Ventura, *J. Am. Chem. Soc.* **1997**, *119*, 12114–12124; b) N. Armaroli, V. Balzani, J.-P. Collin, P. Gavina, J.-P. Sauvage, B. Ventura, *J. Am. Chem. Soc.* **1999**, *121*, 4397–4408.

[13] H. Murakami, A. Kawabuchi, K. Kotto, M. Kunitake, N. Nakashima, *J. Am. Chem. Soc.* **1997**, *119*, 7605–7606.

[14] E. L. Piatnitsky, K. D. Deshayes, *Angew. Chem.* **1998**, *110*, 1022–1024; *Angew. Chem. Int. Ed.* **1998**, *37*, 970–972.

[15] M. Takeshita, M. Irie, *J. Org. Chem.* **1998**, *63*, 6643–6649.

[16] G. Steinberg-Yfrach, J.-L. Rigaud, E. N. Durantini, A. L. Moore, D. Gust, T. A. Moore, *Nature*, **1998**, *392*, 479–482.

[17] Y.-Z. Hu, S. H. Bossmann, D. van Loyen, O. Schwarz, H. Dürr, *Chem. Eur. J.* **1999**, *5*, 1267–1277.

[18] X. Y. Lauteslager, I. H. M. van Stokkum, H. J. Ramesdonk, A. M. Bouwer, J. W. Verhoeven, *J. Phys. Chem. A* **1999**, *103*, 653–659.

[19] N. Koumura, R. W. J. Ziylstra, R. A. van Delden, H. Harada, B. L. Feringa, *Nature* **1999**, *401*, 152–155.

[20] a) A. P. de Silva, H. Q. N. Gunaratne, C. P. McCoy, *Nature* **1993**, *364*, 42–44; b) A. P. de Silva, H. Q. N. Gunaratne, T. Gunnlaugsson, A. J. M. Huxley, C. P. McCoy, J. T. Rademacher, T. E. Rice, *Chem. Rev.* **1997**, *97*, 1515–1566; c) A. Credi, V. Balzani, S. J. Langford, J. F. Stoddart, *J. Am. Chem. Soc.* **1997**, *119*, 2679–2681; d) F. Pina, A. Roque, M. J. Melo, M. Maestri, L. Belladelli, V. Balzani, *Chem. Eur. J.* **1998**, *4*, 1184–1191; e) A. P. de Silva, H. Q. N. Gunaratne, C. P. McCoy, *J. Am. Chem. Soc.* **1999**, *121*, 1393–1394.

[21] M. Gómez-López, J. A. Preece, J. F. Stoddart, *Nanotechnology*, **1996**, *7*, 183–192.

[22] V. Balzani, A. Credi, M. Venturi, in *Supramolecular Science*: *Where It Is and Where It Is Going* (Eds.: R. Ungaro, E. Dalcanale) Kluwer, Dordrecht, **1999**, pp. 1–22.

[23] P. R. Ashton, D. Philp, N. Spencer, J. F. Stoddart, *J. Chem. Soc. Chem. Commun.* **1992**, 1124–1128.

[24] a) K. Kalyanasundaram, *Photochemistry of Polypyridine and Porphyrin Complexes*, Academic Press, London (UK) **1991**; b) E. Amouyal, *Sol. Energy Mater. Sol. Cells* **1995**, *38*, 249–276.

[25] a) A. Juris, V. Balzani, F. Barigelletti, S. Campagna, P. Belser, A. von Zelewsky, *Coord. Chem. Rev.* **1988**, *84*, 85–277; b) V. Balzani, A.

[26] Juris, M. Venturi, S. Campagna, S. Serroni, *Chem. Rev.* **1996**, *96*, 759–833.

[26] We have advocated (M. C. T. Fyfe, P. T. Glink, S. Menzer, J. F. Stoddart, A. J. P. White, D. J. Williams, *Angew. Chem.* **1997**, *109*, 2158–2160; *Angew. Chem. Int. Ed. Engl.* **1997**, *36*, 2068–2070) the use of the term *co-conformation* to designate the different three-dimensional spatial arrangements of a) the constituent parts (e. g., host and guest) in supramolecular systems and b) the components of interlocked molecular systems.

[27] a) E. H. Yonemoto, G. B. Saupe, R. H. Schmehl, S. M. Hubig, R. L. Riley, B. L. Iverson, T. E. Mallouk, *J. Am. Chem. Soc.* **1994**, *116*, 4786–4795; b) E. H. Yonemoto, R. L. Riley, Y. I. Kim, S. J. Atherton, R. H. Schmehl, T. E. Mallouk, *J. Am. Chem. Soc.* **1992**, *114*, 8081–8087.

[28] L. A. Kelly, M. A. J. Rodgers, *J. Phys. Chem.* **1995**, *99*, 13132–13140.

[29] We have used the fully substituted $[Ru(Me_2bpy)_3]^{2+}$ complex $\mathbf{5}^{2+}$ in the place of the more common $[Ru(bpy)_3]^{2+}$ so that when the complex is connected to the spacer, the light-promoted electron in the metal-to-ligand charge-transfer excited state does not preferentially reside on the external ligands. See ref. [28].

[30] a) F. M. Raymo, J. F. Stoddart, *Pure Appl. Chem.* **1997**, *9*, 1987–1997; b) P. R. Ashton, I. Baxter, M. C. T. Fyfe, F. M. Raymo, N. Spencer, J. F. Stoddart, A. J. P. White, D. J. Williams, *J. Am. Chem. Soc.* **1998**, *120*, 2297–2307; c) F. M. Raymo, K. N. Houk, J. F. Stoddart, *J. Am. Chem. Soc.* **1998**, *120*, 9318–9322.

[31] J. L. Sessler, B. Wang, A. Harriman, *J. Am. Chem. Soc.* **1995**, *117*, 704–714.

[32] N. Miyaura, T. Yangi, A. Suzuki, *Synth. Commun.* **1981**, *11*, 513–519.

[33] F. Jannasch, *Z. Chem.* **1870**, 162.

[34] C. G. Griggs, D. J. H. Smith, *J. Chem. Soc. Perkin Trans. I* **1982**, 3041–3043.

[35] P. Lay, A. M. Sargeson, H. Taube, *Inorg. Synth.* **1986**, *24*, 292–293.

[36] P. R. Ashton, R. Ballardini, V. Balzani, M. Belohradsky, M. T. Gandolfi, D. Philp, L. Prodi, F. M. Raymo. M. Reddington, N. Spencer, J. F. Stoddart, M. Venturi, D. J. Williams, *J. Am. Chem. Soc.* **1996**, *118*, 4931–4951.

[37] J. Rebek, Jr., T. Costello, R. Wattley, *J. Am. Chem. Soc.* **1985**, *107*, 7487–7493.

[38] M. Asakawa, P. R. Ashton, R. Ballardini, V. Balzani, M. Belohradsky, M. T. Gandolfi, O. Kocian, L. Prodi, F. M. Raymo, J. F. Stoddart, M. Venturi, *J. Am. Chem. Soc.* **1997**, *119*, 302–310.

[39] Unpublished results. The methyl groups at the 3-and 3′-positions on the bipyridinium unit prevent the ring system from adopting a planar geometry.

[40] P. Wardman, *J. Phys. Chem. Ref. Data* **1989**, *18*, 1637–1755.

[41] P. A. Mabrouk, M. S. Wrighton, *Inorg. Chem.* **1986**, *25*, 526–531.

[42] C. K. Mann, K. K. Barnes, *Electrochemical Reactions in Nonaqueous Systems*, Dekker, New York, **1970**.

[43] R. Ballardini, V. Balzani, C. L. Brown, A. Credi, R. E. Gillard, M. Montalti, D. Philp, J. F. Stoddart, M. Venturi, A. J. P. White, B. J. Williams, D. J. Williams, *J. Am. Chem. Soc.* **1997**, *119*, 12503–12513.

[44] The oxidation of the two hydroquinone rings occurs at the same potential because, for symmetry reasons, they are equally affected by the CT interaction and do not interact with each other.

[45] We thank R. Forster and E. Figgemeier (Dublin City University) for having offered us the opportunity to attempt to do these experiments.

[46] M. Z. Hoffmann, F. Bolletta, L. Moggi, G. L. Hug, *J. Phys. Chem. Ref. Data* **1989**, *18*, 219–543.

[47] R. A. Marcus, *Annu. Rev. Phys. Chem.* **1964**, *15*, 155–196.

[48] Excitation in the UV region showed that the potentially fluorescent excited states of ring **R**, spacer **S**, and stopper **T** do not emit in $\mathbf{1}^{6+}$ because of energy or electron transfer quenching processes caused by the other units.

[49] Under the experimental conditions employed (5×10^{-6} to 1×10^{-4} M solutions), the occurrence of dynamic quenching can be ruled out because the luminescence lifetime did not show any concentration dependence.

[50] a) R. Bensasson, C. Salet, V. Balzani, *J. Am. Chem. Soc.* **1976**, *98*, 3722–3723; b) C. Creutz, M. Chou, T. L. Netzel, M. Okumura, N. Sutin, *J. Am. Chem. Soc.* **1980**, *102*, 1309–1319.

[51] In principle, in the case of the [2]rotaxane $\mathbf{1}^{6+}$ an alternative quenching mechanism could have been energy transfer from the excited state of **P** to the donor/acceptor CT excited state arising from the interaction

between the $\mathbf{A_1}$ station and the macrocycle $\mathbf{R}$. In such a case, however, no long-lived transient would have been observed.

[52] Obtained by photochemical reduction of $\mathbf{7}^{2+}$ and $\mathbf{8}^{2+}$ in degassed acetonitrile solution by using $[Ru(bpy)_3]^{2+}$ as a photosensitizer and TEOA as a sacrificial electron donor.

[53] T. Wanatabe, K. Honda, *J. Phys. Chem.* **1982**, *86*, 2617 – 2619.

[54] N. A. McAskill, *Aust. J. Chem.* **1984**, *37*, 1579 – 1592.

[55] D. Gust, T. A. Moore, *Top. Curr. Chem.* **1991**, *159*, 103 – 151.

[56] The thermal shuttling rate of BPP34C10 between two identical 4,4′-bipyridinium stations in a previously studied [2]rotaxane was found to occur with a time constant of 3.3 µs in CD_3COCD_3 at 298 K (ref. [23]). In our case, although the arrival station $\mathbf{A_2}$ is somewhat bulkier, one might expect an even faster displacement rate because the forward electron transfer process deactivates the starting station $\mathbf{A_1}$.

[57] V. Balzani, A. Credi, F. M. Raymo, J. F. Stoddart, *Angew. Chem.* **2000**, *112*; *Angew. Chem. Int. Ed.* **2000**, *112*, in press.

[58] The term *molecular shuttle* was introduced in 1991 to describe a [2]rotaxane with two identical stations on its dumbbell-shaped component between which one ring component shuttled back and forth in a degenerate manner. See: P. L. Anelli, N. Spencer, J. F. Stoddart, *J. Am. Chem. Soc.* **1991**, *113*, 5131 – 5133. Desymmetrization of the dumbbell-shaped component led to [2]rotaxanes that exhibited translational isomerism between two isomers with finite populations. See: P. L. Anelli, M. Asakawa, P. R. Ashton, R. A. Bissell, G. Clavier, R. Górski, A. E. Kaifer, S. J. Langford, G. Mattersteig, S. Menzer, A. M. Z. Slawin, N. Spencer, J. F. Stoddart, M. S. Tolley, D. J. Williams, *Chem. Eur. J.* **1997**, *3*, 1113 – 1135. Subsequently, one of these desymmetrized [2]rotaxanes had its molecular shuttling controlled both chemically and electrochemically. See: R. A. Bissell, E. Córdova, A. E. Kaifer, J. F. Stoddart, *Nature*, **1994**, *369*, 133 – 137. Thereafter, by employing two very different recognition motifs, molecular shuttles that could be switched chemically between one state and another ($\sim 100 : \sim 0 \rightarrow \sim 0 : \sim 100$) were realized. See: a) M.-V. Martínez-Díaz, N. Spencer, J. F. Stoddart, *Angew. Chem.* **1997**, *109*, 1991 – 1994; *Angew. Chem. Int. Ed. Engl.* **1997**, *36*, 1904 – 1907; b) P. R. Ashton, R. Ballardini, V. Balzani, I. Baxter, A. Credi, M. C. T. Fyfe, M.-T. Gandolfi, M. Gómez-López, M.-V. Martínez-Díaz, A. Piersanti, N. Spencer, J. F. Stoddart, M. Venturi, A. J. P. White, D. J. Williams, *J. Am. Chem. Soc.* **1998**, *120*, 11 932 – 11 942.

[59] P. L. Anelli, P. R. Ashton, R. Ballardini, V. Balzani, M. Delgado, M. T. Gandolfi, T. T. Goodnow, A. E. Kaifer, D. Philp, M. Pietraszkiewicz, L. Prodi, M. V. Reddington, A. M. Z. Slawin, N. Spencer, J. F. Stoddart, C. Vicent, D. J. Williams, *J. Am. Chem. Soc.* **1992**, *114*, 193 – 218.

[60] D. D. Perrin, W. F. L. Armarego, *Purification of Laboratory Chemicals*, Pergamon, Oxford, **1989**.

[61] J. N. Demas, G. A. Crosby, *J. Phys. Chem.* **1971**, *75*, 991 – 1024.

[62] K. Nakamaru, *Bull. Chem. Soc. Jpn.* **1982**, *55*, 2697 – 2705.